Balance Between EGF/STAT1 and IFNγ/NRF2 Signaling Controls ECM1 Expression and Determines Hepatic Homeostasis versus Chronic Liver Disease

Yujia Li[1], Chenjun Huang[1, 2], Weiguo Fan[3], Seddik Hammad[1], Lea Berger[4, 5], Cyrill Géraud[4, 5, 6], Ye Yao[1], Frederik Link[1], Chenhao Tong[1], Zeribe C. Nwosu[1, 7], Pia Erdösi[1], Weronika Piorońska[1], Kerry Gould[1], Christoph Meyer[1], Rilu Feng[1, 8], Hui Liu[9], Chen Shao[9], Bing Sun[10], Huiguo Ding[11], Roman Liebe[12], Matthias P. A. Ebert[1, 13, 14], Honglei Weng[1], Chunfang Gao[2], Peter ten Dijke[15], Steven Dooley[1*], and Sai Wang[1*]

[1] Department of Medicine II, University Medical Center Mannheim, Medical Faculty Mannheim, Heidelberg University, Mannheim, Germany;

[2] Department of Clinical Laboratory Medicine Center, Yueyang Hospital of Integrated Traditional Chinese and Western Medicine, Shanghai University of Traditional Chinese Medicine, Shanghai, China;

[3] Key Laboratory of Multi-Cell Systems, Shanghai Institute of Biochemistry and Cell Biology, Center for Excellence in Molecular Cell Science, Chinese Academy of Sciences, Shanghai, China;

[4] Section of Clinical and Molecular Dermatology, Department of Dermatology, Venereology, and Allergology, University Medical Center and Medical Faculty Mannheim, Heidelberg University, Mannheim, Germany;

[5] European Center for Angioscience, Medical Faculty Mannheim, Heidelberg University, Mannheim, Germany;

[6] DKFZ Hector Cancer Institute at the University Medical Center Mannheim, Mannheim, Germany;

[7] Department of Molecular Biology and Genetics, Cornell University, Ithaca, NY, USA;

[8] Department of Endocrinology and Metabolism, Renji Hospital, School of Medicine, Shanghai Jiao Tong University, Shanghai, China;

[9] Department of Pathology, Beijing You'an Hospital, Affiliated with Capital Medical University, Beijing, China;

[10] State Key Laboratory of Cell Biology, Shanghai Institute of Biochemistry and Cell Biology, Center for Excellence in Molecular Cell Science, Chinese Academy of Sciences, Shanghai, China;

[11] Department of Gastroenterology and Hepatology, Beijing You'an Hospital, Affiliated with Capital Medical University, Beijing, China;

[12] Clinic of Gastroenterology, Hepatology and Infectious Diseases, Otto-von-Guericke-University, Magdeburg, Germany;

[13] Molecular Medicine Partnership Unit, European Molecular Biology Laboratory, Heidelberg, Germany;

[14] DKFZ-Hector Cancer Institute at the University Medical Center, Mannheim, Germany;

[15] Oncode Institute and Department of Cell and Chemical Biology, Leiden University Medical Center, Leiden, Netherlands.

Corresponding author:

Prof. Dr. rer. nat. Steven Dooley

Department of Medicine II, Section Molecular Hepatology, University Medical Center Mannheim, Medical Faculty Mannheim, Heidelberg University

Theodor-Kutzer-Ufer 1-3

68167 Mannheim, Germany

Email: steven.dooley@medma.uni-heidelberg.de

Tel: +49-621-383-3768

Dr. sc. hum. Sai Wang

Department of Medicine II, Section Molecular Hepatology, University Medical Center Mannheim, Medical Faculty Mannheim, Heidelberg University

Theodor-Kutzer-Ufer 1-3

68167 Mannheim, Germany

Email: sai.wang@medma.uni-heidelberg.de

Tel: +49-621-383-5595

Number of figures and tables: 7 figures

Financial support

This work was supported by the Deutsche Forschungsgemeinschaft (DFG) [grant number DO 373/20-1 to SD], Federal Ministry of Education and Research (BMBF) Program LiSyM-HCC, [grant number PTJ-031L0257A to SD], the Stiftung Biomedizinische Alkohol-Forschung, [grant number 73000350], and HiChol [01GM1904A to RL].

Author contributions

Conceptualization: SD, SW

Methodology: YL, SW, WF, CH, SH, CT, ZCN, YY, PE, WP, KG, RF, HL, CS

Investigation: YL, SW, CH, WF, SH, YY, FL, CT, ZCN, LB, CG, PE, CM, HL, CS

Visualization: YL, SW, CH

Funding acquisition: SD

Project administration: SD, SW, YL

Supervision: SW, SD

Writing - Original: YL, SW, SD

Writing - review: YL, SW, SD, PTD, RL, CH, FL, ZCN, CM, BS, HD, ME, CG, HW

SW and SD acted as guarantors.

Abstract

In healthy livers, extracellular matrix protein 1 (ECM1) is essential for liver homeostasis by keeping latent transforming growth factor-β (LTGF-β) quiescent. Upon hepatocyte damage, ECM1 is downregulated, facilitating LTGF-β activation and fibrogenesis. However, little is known about how hepatic ECM1 is regulated. Here we found in healthy hepatocytes, EGF/EGFR signaling sustains ECM1 expression through phosphorylating STAT1 at S727, enhancing its binding to the *ECM1* promoter and boosting gene transcription. During liver inflammation, accumulating IFNγ disrupts this process by downregulating EGFR and inhibiting EGF/EGFR/STAT1-mediated *ECM1* promoter binding. Mechanistically, IFNγ-induced STAT1 phosphorylation at Y701 impairs the binding of p-STAT1 S727 to the ECM1 promoter. Additionally, IFNγ induces NRF2 nuclear translocation, which repressively binds to the *ECM1* promoter, further reducing its expression. These findings were confirmed in several chronic liver disease (CLD) mouse models. Moreover, AAV8-ECM1 significantly attenuates liver fibrosis and injuries in Western diet (WD)-fed mice. Notably, in patients with CLD, ECM1 levels align with EGFR expression, while NRF2 and LTGF-β activation show a negative correlation with both.

166 words

Keywords: ECM1, EGF, IFNγ, TGF-β, liver fibrosis

92 **Introduction**

93 Extracellular matrix protein 1 (ECM1) is a secreted 85-kDa glycoprotein (Mathieu *et*
94 *al*, 1994) primarily found in the epidermis and dermis (Smits *et al*, 2000), where it
95 functions to maintain the integrity and homeostasis of the skin (Sercu *et al*, 2009).
96 ECM1 is also involved in the development of cancer and its levels are elevated in most
97 malignant epithelial and metastatic tumours, including breast cancer, colon cancer,
98 ovarian cancer, and melanoma (Sercu *et al*, 2008; Wang *et al*, 2003). In contrast, in our
99 previous studies, we identified ECM1 as gatekeeper of liver homeostasis by interacting
100 with and inhibiting αv integrin-, thrombospondin 1 (TSP-1)-, ADAMTS protease 1
101 (ADAMTS1)-, and matrix metalloproteinase (MMP)-mediated latent TGF-β (LTGF-β)
102 activation (Fan *et al*, 2019; Li *et al*, 2022; Link *et al*, 2024). Mice lacking *Ecm1* gene
103 display severe hepatic fibrosis and die between ages of 8 to 12 weeks (Fan *et al.*, 2019).
104 ECM1 is produced mainly by hepatocytes and quiescent hepatic stellate cells (HSCs),
105 deposited in the extracellular matrix for its function (Fan *et al.*, 2019; Filliol *et al*, 2022).
106 Importantly, ECM1 expression is significantly downregulated following hepatocyte
107 injury and HSC activation (Fan *et al.*, 2019). However, since hepatocytes are the most
108 vulnerable cells in the liver (Gribben *et al*, 2024), the reduction of ECM1 mediated by
109 damaged hepatocytes, especially at the early stages of chronic liver disease (CLD) prior
110 to HSC activation, is considered a key factor in initiating further liver injuries (Fan *et*
111 *al.*, 2019).

112 Several tested mouse models of liver disease e.g., carbon tetrachloride (CCl_4)-,
113 metabolic dysfunction-associated steatohepatitis (MASH)-, and bile duct ligation
114 (BDL)-associated liver injury consistently display Ecm1 downregulation (Fan *et al.*,
115 2019), suggesting a common initiating mechanism of liver fibrogenesis. A progressive
116 loss of ECM1 with disease severity is present in patients with liver fibrosis/cirrhosis
117 (Fan *et al.*, 2019), and this also correlates with poorer prognosis in hepatocellular
118 carcinoma (HCC) patients (Bai *et al*, 2020; Gao *et al*, 2014). It is therefore of great
119 interest to investigate ECM1 expression regulation in the liver context. Our research

120 focused on the regulation of ECM1 expression in hepatocytes, as they are one of the
121 main producers and the downregulation of ECM1 by injured hepatocytes in the early
122 stages of CLD is a crucial factor in driving disease progression.

123 **Results**

124 **EGF promotes ECM1 expression in hepatocytes**

125 As reported previously, hepatic ECM1 expression undergoes a significant
126 downregulation in response to liver injury (Fan *et al.*, 2019). To gain a comprehensive
127 understanding of its modulation in liver pathology, we analyzed the *ECM1* mRNA
128 expression in liver tissue of CLD patients sourced from the Gene Expression Omnibus
129 (GEO) online database. It revealed a consistent reduction in *ECM1* expression across
130 various cohorts of CLD patients, demonstrating a correlation with disease progression
131 **(Figure 1A)**. Specifically, this decline was evident in patients with metabolic
132 dysfunction-associated steatotic liver disease (MASLD, n=15) and metabolic
133 dysfunction-associated steatohepatitis (MASH, n=16), in comparison to healthy
134 individuals with normal weight (n=14) and obesity (n=12) (Suppli *et al*, 2019) **(Figure**
135 **1A, left)**. Furthermore, *ECM1* expression was notably diminished in alcoholic cirrhosis
136 patients (n=67) relative to those with non-severe alcoholic hepatitis (n=13) and
137 alcoholic steatosis (n=6) (Trepo *et al*, 2018) **(Figure 1A, middle)**. In addition, the
138 observed significant decrease in *ECM1* mRNA expression extended to tumor tissue
139 from HBV-associated HCC patients (n=21) compared to non-neoplastic liver tissues
140 (Yoo *et al*, 2017) **(Figure 1A, right)**. This consistent pattern underscores the potential
141 role of ECM1 in the pathogenesis and progression of various liver diseases.

142 Our previous study demonstrated that healthy hepatocytes are one of the primary
143 producers of ECM1 in the liver, as identified through qRT-PCR and immunoblotting
144 (Fan *et al.*, 2019). To further confirm the specific role of hepatocytes in maintaining
145 ECM1 expression, we analyzed several scRNA-seq datasets from various mouse
146 models of liver injury and patients with CLD. In 3,5-diethoxycarbonyl-1,4-

147 dihydrocollidine (DDC) diet-injured mouse model (GSE193850) (Li *et al*, 2023), we
148 classified the cell clusters into diverse categories **(Figure 1B, first panel)** based on the
149 marker genes **(Suppl. Fig. 1A)**, among others, InjuredHeps and NormalHeps were
150 selected for further analysis **(Figure 1B, second panel)**. Heatmap showed that in the
151 injured hepatocytes, the expression of *Ecm1* was significantly deseased as compared to
152 normal hepatocytes **(Figure 1B, third panel)**. Similarly, *Ecm1* expression in
153 hepatocytes was also reduced in choline-deficient high-fat diet (CD-HFD)-fed mice
154 (GSE232182) compared to the control diet **(Suppl. Fig. 1B; Figure 1C)**. Furthermore,
155 in CLD patients (GSE202379) (Gribben *et al.*, 2024), as the MASLD/MASH
156 developed, the expression of *ECM1* in hepatocytes likewise progressively declined
157 relative to healthy donors **(Suppl. Fig. 1C; Figure 1D)**. Since hepatocytes are the cell
158 type most affected by the disease and exhibit a significant downregulation of ECM1
159 expression before HSC activation upon liver injury (Fan *et al.*, 2019; Gribben *et al.*,
160 2024), this suggests that the reduction in ECM1 by injured hepatocytes may be a key
161 factor contributing to CLD progression. Therefore, our study focuses on investigating
162 the mechanisms underlying ECM1 regulation in hepatocytes.
163 To get a broader understanding of signaling pathways and transcription factors
164 potentially implicated in the regulation of *Ecm1* transcription, we performed an *in silico*
165 analysis of the *Ecm1* gene (NCBI Gene ID: 13601) promoter (-2000bp ~ +200bp
166 relative to transcription start site (TSS)) using PROMO (https://alggen.lsi.upc.es/cgi-
167 bin/promo_v3/promo/promoinit.cgi?dirDB=TF_8.3), GeneCards (ECM1 Gene -
168 GeneCards) and JASPAR (https://jaspar.genereg.net/), and identified multiple binding
169 sites for candidate transcription factors, including, among others, Fos, Jun, cMyc, NF-
170 κB, and Stat1 **(Suppl. Fig. 2)**. NF-κB is mainly regulated by inflammatory cell
171 signaling induced by TNF-α and LPS. Fos, Jun, cMyc, and Stat1 are downstream
172 transcription factors of growth factors, especially EGF and HGF. Additionally, Stat1 is
173 a major downstream mediator of the interferon family. As these signaling molecules all

174 are having prominent roles in liver physiology and pathophysiology, they are promising
175 candidates as crucial regulators of hepatic Ecm1 expression.
176 Next, we tested previously described pathways for their impact on *Ecm1* mRNA
177 expression levels. 4ng/ml TNF-α or 5µg/ml LPS treatment did not impact on *Ecm1*
178 mRNA expression in mouse primary hepatocytes (MPHs) **(Suppl. Fig. 3)**; EGF and
179 HGF treatment consistently induced *ECM1* expression on mRNA levels in MPHs,
180 human primary hepatocytes (HPHs) and AML12 cells **(Figure 1E**, **Suppl. Fig. 4A)**, as
181 well as promoted Ecm1 protein expression in MPHs **(Figure 1F)** and AML12 cells
182 **(Suppl. Fig. 4B)**.

183 **EGF/EGFR signaling contributes to physiological Ecm1 expression in liver**
184 **homeostasis**

185 Given the crucial role of the EGFR in the EGF signaling pathway (Zeineldin & Hudson,
186 2006), we applied erlotinib, a selective EGFR inhibitor in EGF-treated AML12 cells
187 and MPHs. qRT-PCR and Western blotting analysis confirmed that erlotinib
188 substantially inhibited EGF-induced Egfr phosphorylation and Ecm1 expression in both
189 cell systems **(Figure 1G; Suppl. Fig. 4C)**. In line, siRNA mediated *Egfr* knockdown
190 as well suppressed Egfr expression/phosphorylation levels, and Ecm1 expression in
191 MPHs upon treatment with EGF **(Figure 1H)**. To confirm our findings *in vivo*, EGF
192 was injected to WT mice through tail vein (200µg/kg body weight (BW)). Results
193 showed that EGF treatment did not increase Ecm1 expression *in vivo*, which might be
194 due to the physiological level of EGF in the healthy liver **(Suppl. Fig. 5)**. Alternatively,
195 we applied erlotinib (40mg/kg BW, for 2 days) to WT mice intraperitoneally (i.p.) and
196 analysed the liver tissue 48hrs later. qRT-PCR, Western blotting, and
197 immunofluorescence (IF) analysis showed a significant decrease in Ecm1 expression
198 in the erlotinib-treated group compared to the control group **(Figure 1I, J)**. Further
199 evidence of this downregulation was demonstrated in Ecm1-tdTomato transgenic mice.
200 In the liver tissue of these mice, Ecm1 was visualized by tdTomato fluorescence, which

201 showed a reduction in red florescence signal under the same erlotinib treatment
202 conditions **(Figure 1K)**. Consistent with our previous finding that ECM1 loss leads to
203 the activation of latent TGF-β1 (LTGF-β1), erlotinib injection significantly activated
204 LTGF-β1, as indicated by the elevated expression of LAP-D R58, a breakdown product
205 of the TGF-β1 latency-associated peptide (LAP) that is detectable in the ECM upon
206 LTGF-β1 activation (**Figure 1L**).
207 These results suggest that constant/basal EGF-EGFR signaling maintains Ecm1
208 expression in healthy livers.

209 **EGF induces Ecm1 expression through Stat1**

210 To elucidate potential downstream components of the EGF-EGFR signaling pathway
211 that regulate Ecm1 expression, we tested several transcription factors as predicted from
212 the *in silico* promoter study, such as Fos, Jun, cMyc, and Stat1, together with its major
213 downstream Erk signaling, by depleting their availability with siRNA interference
214 experiments. Knockdown of Fos, Jun, or cMyc, Erk1 and Erk2 did not interfere with
215 EGF-induced Ecm1 expression **(Suppl. Fig. 6A-E),** whereas qRT-PCR and
216 immunoblot data revealed that *Stat1* silencing by siRNA markedly suppressed EGF-
217 induced Ecm1 expression in MPHs **(Figure 2A)** and AML12 cells **(Suppl. Fig. 7A)**.
218 This suggested Stat1 as a promising candidate. In line, 1hr EGF treatment of MPHs
219 induced phosphorylation of Stat1 at S727 phosphorylation site, which remained stable
220 for at least 24hrs **(Figure 2B)**. As Stat1 is also an EGF-EGFR downstream target
221 (Wang, 2017), its total expression and phosphorylation at S727 were measured in EGF-
222 treated MPHs with or without siRNA targeting *Egfr*. Western blotting showed EGF-
223 induced total expression and phosphorylation of Stat1 to be dependent on Egfr **(Figure**
224 **2C)**. Notably, Egfr inactivation also inhibited the phosphorylation of Stat1 at position
225 S727 in the mice treated with erlotinib **(Figure 2D)**. Preliminary data on HGF signaling,
226 showing that depleting Stat1 did not abrogate Ecm1 expression induction in MPHs,

227 suggest involvement of alternate pathways, whose detailed delineation is subject matter
228 of an ongoing investigation **(Suppl. Fig. 8)**.
229 Next, we studied whether Stat1 overexpression is sufficient to upregulate Ecm1.
230 Therefore, we transfected AML12 cells with eGFP-Stat1 and eGFP plasmids,
231 respectively. Western blotting revealed that overexpression of Stat1 increased total
232 Stat1 expression, Stat1 phosphorylation at position S727, and Ecm1 expression **(Figure**
233 **2E)**. These data consistently demonstrate that Stat1 is required for EGF-EGFR-
234 mediated signal transduction towards Ecm1 expression in hepatocytes.

235 **EGF induces Stat1 binding to the *Ecm1* promoter for its transcriptional activation**
236 We predicted the binding of Stat1 to the *Ecm1* promoter using JASPAR
237 (https://jaspar.genereg.net/), which showed a putative binding motif
238 ATGGCAGGAAA at -59 ~ -49bp to the *Ecm1* TSS **(Figure 2F)**. To investigate the
239 regulatory role of Stat1 in *Ecm1* transcription, we constructed a luciferase reporter
240 plasmid containing the corresponding *Ecm1* promoter region (-339 ~ +161bp) and
241 transfected it into HEK293T cells. Overexpression of Stat1 remarkably increased
242 luciferase activity of the reporter construct **(Figure 2G)**, suggesting that Stat1 binding
243 to the *Ecm1* promoter directly regulates gene transcription. Next, we functionally
244 validated the binding of Stat1 to the predicted binding motif located in the *Ecm1* gene
245 promoter region between -155bp and +120bp in MPHs by chromatin
246 immunoprecipitation (ChIP) qRT-PCR experiments, and the constitutive binding
247 activity was significantly increased by EGF treatment **(Figure 2H)**. The ChIP PCR-
248 amplified products were visualized on 2% agarose gel **(Figure 2I).** Similar results were
249 also obtained in AML12 cells **(Suppl. Fig. 7B, C)**.
250 These results indicate that EGF induces binding of Stat1 to the proximal promoter
251 region (typically within 250bp upstream of the TSS) of the *Ecm1* gene, thereby
252 activating its transcription.

253 **IFNγ inhibits EGF/EGFR-mediated Ecm1 expression**

254 IFNγ is a strong modulator of Stat1 signaling (Platanias, 2005) and is found to inhibit
255 HSC activation (Weng *et al*, 2007) but induce hepatocyte apoptosis and hepatic
256 inflammation in CLD (Horras *et al*, 2011). This prompts us to investigate how IFNγ
257 regulates Ecm1 expression in hepatocytes. Treatment of MPHs with IFNγ decreased
258 Ecm1 expression on mRNA and protein levels **(Figure 3A)**. Moreover, IFNγ abrogated
259 EGF-induced Egfr activation and Ecm1 expression, as determined by qRT-PCR and
260 immunoblotting analysis **(Figure 3A)**. EGF and IFNγ can activate Stat1 pathway, but
261 the outcome in the hepatocytes is distinct between them. Although EGF and IFNγ both
262 phosphorylate Stat1 at S727, the difference is that IFNγ requires phosphorylation at
263 Y701 prior to the S727 phosphorylation event (Sadzak *et al*, 2008), whereas EGF is
264 able to directly phosphorylate Stat1 at S727 via EGFR (Zhang *et al*, 2004). In detail,
265 immunoblot analysis of lysates from MPHs treated with EGF or IFNγ for different time
266 intervals displayed that IFNγ induced phosphorylation of Stat1 at Y701 within 5min,
267 which was followed by phosphorylation of S727 at between 10 to 30min **(Figure 3B)**.
268 In contrast, EGF-mediated S727 phosphorylation of Stat1 arose rapidly, whereas Y701
269 phosphorylation did not take place **(Figure 3B)**. Furthermore, EGF transiently induced
270 Egfr phosphorylation at Y1068 within 5min, therewith initiating its downstream
271 signaling towards Stat1. Moreover, IFNγ inhibits total Egfr expression and was not able
272 to activate Egfr **(Figure 3B)**. ChIP qRT-PCR experiments indicated that IFNγ treatment
273 did not increase Stat1 binding to the *Ecm1* gene promoter in MPHs **(Figure 3C)**. This
274 suggests that unlike Stat1 phosphorylated at S727 alone, Stat1 phosphorylated at both
275 Y701 and S727 cannot bind to the *Ecm1* gene promoter to induce its transcription.
276 Moreover, the addition of IFNγ significantly reduced EGF-induced binding of Stat1 to
277 the *Ecm1* gene promoter as evidenced by the fold enrichment in the ChIP assay **(Figure
278 3D)**. Next, we administered IFNγ to mice via i.p. injection (400μg/kg BW, for 4 days).
279 Expression of Ecm1 and Egfr were significantly reduced in the IFNγ-treated group
280 compared to controls, as determined by qRT-PCR and immunoblotting **(Figure 3E)**.

281 The decrease in Ecm1 expression was further confirmed by IF staining **(Figure 3F)**.
282 Additionally, Ecm1 was markedly reduced in Ecm1-tdTomato transgenic mice, as
283 observed by tdTomato fluorescence under the same IFNγ treatment conditions **(Figure**
284 **3G)**. In line with our hypothesis, IFNγ injection also enhanced LAP-D R58 staining in
285 the liver tissue (**Figure 3H**), indicating upregulated LTGF-β1 activation. Finally,
286 increased expression of fibrotic markers *Acta2*, *Timp1*, *Mmp9*, and *Col1a1* was present
287 in livers of IFNγ-injected mice (**Figure 3I**).
288 In conclusion, these results imply that IFNγ disrupts Ecm1 homeostasis maintained by
289 EGF-EGFR signaling through inhibiting Egfr expression, and blocks binding of p-Stat1
290 S727 to the *Ecm1* gene promoter by phosphorylating Stat1 at Y701.

291 **IFNγ inhibits Ecm1 expression through Nrf2 activation**

292 In CLD, IFNγ promotes inflammation and induces ROS (Lee *et al*, 2007; Miyawaki *et*
293 *al*, 2019), which leads to Nrf2 activation (Jaeschke & Woolbright, 2012). The *in silico*
294 analysis predicted Nrf2 binding sites at the *Ecm1* gene promoter, indicating Nrf2 may
295 negatively regulate *Ecm1* transcription. Consistent with current knowledge, IFNγ
296 treatment induced ROS-related gene expression, such as *Nos2*, *Cybb*, *Nrf2*, *Nqo1*,
297 *Hmox1*, and *Nox4*, both in cultured cells and in mice **(Figure 4A-B)**. Upregulated ROS
298 gene expression also indicates increased ROS activity, as measured by the fluorescent
299 H2DCFDA, which is converted by intracellular oxidation (488/525 nm) in MPHs
300 treated with IFNγ **(Figure 4C)**. Finally, IF staining of tissue sections demonstrated
301 nuclear accumulation of Nrf2 in the livers of IFNγ-treated mice **(Figure 4D),** however,
302 no differences for total Nrf2 protein expression were evident based on immunoblots
303 **(Suppl. Fig. 9A)**. Next, we treated MPHs with EGF and/or IFNγ and prepared nuclear
304 and cytoplasmic lysates for immunoblot analysis. It shows that the Nrf2 signal in the
305 nuclear fraction was strongly induced upon IFNγ treatment **(Figure 4E)**. IFNγ
306 dependent Nrf2 nuclear accumulation in MPHs was additionally confirmed by IF
307 staining for Nrf2 **(Figure 4F)**. To further investigate whether IFNγ-mediated Ecm1

308 downregulation is dependent on Nrf2, we depleted Nrf2 with RNAi in the setting of
309 IFNγ treatment in MPHs **(Suppl. Fig. 9B)**. The data shows that Nrf2 knockdown
310 rescued IFNγ-mediated Ecm1 downregulation **(Figure 4G)**.
311 Given that Nrf2 is activated by ROS (Jaeschke & Woolbright, 2012), we treated MPHs
312 with hydrogen peroxide (H_2O_2) to directly induce oxidative stress. With this
313 experiment, we demonstrated an alternative route of ROS-mediated Nrf2 activation
314 with the same effect on Ecm1 mRNA and protein expression downregulation **(Figure**
315 **4H, I)**. Depleting Nrf2 in this setting (**Suppl. Fig. 9C)** rescued the H_2O_2-mediated
316 Ecm1 downregulation **(Figure 4J)**. In addition, H_2O_2 inhibited EGF-induced Y1068
317 phosphorylation of the Egfr, S727 phosphorylation of Stat1, total Stat1-, as well as
318 Ecm1 expression **(Figure 4K)**. Bright field photos of MPH treated with H_2O_2 indicate
319 that the cells were in good conditions during the experiment **(Suppl. Fig. 9D)**,
320 excluding the assumption that the observed effects are relying on cellular damage.
321 These results together suggest that IFNγ inhibits Ecm1 expression in hepatocytes
322 through Nrf2 activation. Given its potential to bind the *Ecm1* promoter, Nrf2 is a
323 candidate regulator for *Ecm1* transcription modulation.

324 **Nrf2 inhibits Ecm1 expression through negative regulatory binding to its**
325 **promoter**

326 To further confirm the inhibitory effect of Nrf2 on Ecm1 expression, we used a specific
327 agonist of Nrf2, Oltipraz (OPZ). The data showed that OPZ, as expected, promoted
328 Nrf2 expression on mRNA and protein levels **(Figure 5A)** and induced its nuclear
329 accumulation in MPHs **(Figure 5B)**. Ecm1 expression was significantly downregulated
330 upon OPZ treatment in MPHs **(Figure 5C)**. Importantly, knockdown of Nrf2
331 effectively mitigated the OPZ-induced reduction on Ecm1 levels **(Figure 5D),**
332 suggesting that despite several other known functions of OPZ, the observed effects are
333 specifically relying on stabilizing Nrf2. Further, the OPZ treatment effects could be
334 phenocopied by Nrf2 overexpression, which as well prevented EGF-induced Ecm1

335 expression **(Figure 5E)**. Finally, OPZ-mediated Nrf2 activation was able to abrogate
336 EGF-driven upregulation of Ecm1 expression **(Figure 5F)**.
337 To investigate whether Nrf2 prevented *Ecm1* expression through its transcription
338 inhibition, we constructed a luciferase reporter plasmid comprising *Ecm1* promoter (-
339 953 ~ -454bp), which contained the predicted Nrf2 binding site at positions -608 ~ -
340 594bp of the *Ecm1* gene promoter (**Figure 5G**, predicted binding motif antisense
341 GGACATGACTCAGAA) and was transfected into HEK293T cells. Overexpression
342 of Nrf2 markedly reduced the luciferase activity of the reporter construct **(Figure 5H)**,
343 indicating that Nrf2 directly and negatively regulates the *Ecm1* promoter. We next
344 performed ChIP qRT-PCR for the region -865bp to -586bp of *Ecm1* gene promoter, in
345 OPZ-treated MPHs, and functionally proved that OPZ-induced Nrf2 binds directly to
346 the *Ecm1* gene promoter **(Figure 5I)**. Amplification products were visualized on 2%
347 agarose gel **(Figure 5J)**.
348 To validate the effect of Nrf2 on Ecm1 expression *in vivo*, we performed i.p. injection
349 of OPZ (150mg/kg BW) into WT mice once per week for 2 weeks. It showed that OPZ
350 treatment resulted in Ecm1 downregulation at the mRNA and protein levels **(Figure**
351 **5K)**. IF staining confirmed the nuclear translocation of Nrf2, reduction of Ecm1
352 expression, and LTGF-β activation in OPZ-treated mice **(Figure 5L-N)**. Next, we
353 extracted mRNA expression data from GEO dataset GSE134188 (He *et al*, 2020) of the
354 target genes involved in the Ecm1 expression regulation network from a mouse model
355 of hyperactivated Nrf2. Specifically, liver-specific autophagy adaptor p62/Sqstm1
356 (p62)-KO mice were injected with/without adenovirus p62 and were analyzed 7 days
357 after injection. In these mice, p62 expression sequesters inhibitory Kelch-like ECH-
358 associated protein 1 (KEAP1) from Nrf2, which results in activation and subsequent
359 nuclear accumulation of activated Nrf2 (He *et al.*, 2020). The analysis demonstrates
360 that the pro-inflammatory signals (*Ifng*, *Ifngr*, *Tnf*, *Nfkb*, *Il1*, *Il6*, et.al), *Stat1*, and *Nrf2*
361 (*Nfe2l2*) were notably increased, while *Egfr* and *Ecm1* were decreased **(Figure 5O, left**
362 **penal)**. In consequence, TGF-β signaling was hyperactivated, here documented by

363 upregulated expression of *Tgfbr1*, *Ctgf*, and *Pmepa1*, which resulted in HSC activation
364 (upregulated *Acta2*), and fibrogenesis, as evident from upregulated expression of
365 fibrogenic genes (*Col1a1*, *Col1a2*, *Col3a1, Fsp1*) **(Figure 5O, middle penal)** and
366 genes related to extracellular matrix remodelling (*Timp1*, *Integrins*, *Adamts*, *Thbs*,
367 *Mmps*) **(Figure 5O, right penal)**.

368 **Activation of IFNγ/NRF2 signaling and downregulation of EGFR/ECM1 in**
369 **various mouse models of hepatic injury**

370 Given the considerable downregulation of Ecm1 in several mouse models with
371 progressive liver fibrosis (Fan *et al.*, 2019), we further investigated the regulatory
372 network of hepatic Ecm1 expression by evaluating mRNA expression of target genes
373 from the GEO dataset. Mice were challenged with CCl_4 (twice per week for 6 weeks,
374 GSE222576) (Hammad *et al*, 2023) **(Figure 6A)**, underwent surgical BDL (7 days after
375 ligation, GSE166867) (Holland *et al*, 2022) **(Figure 6B)**, knocked out of the *Fxr* gene,
376 which encodes a nuclear receptor regulating bile acid and cholesterol homeostasis
377 (GSE76163) (Ijssennagger *et al*, 2016) **(Figure 6C)**, given 0.1% DDC diet (for 1 week,
378 GSE193850) (Li *et al.*, 2023) **(Figure 6D)**, or fed with CD-HFD (for 3 months,
379 GSE232182) **(Figure 6E)**. Bulk RNA-seq and scRNA-seq analysis illustrated the
380 downregulation of *Ecm1*, *Egfr*, along with the upregulation of *Ifngr1*, *Ifngr2*, *Nfe2l2*
381 and its target genes, including antioxidant enzymes cytochrome P450 family 1
382 subfamily B member 1 (*Cyp1b1*) and NAD(P)H:quinone oxidoreductase 1 (*Nqo1*).
383 Additionally, TGF-β signaling was markedly activated in these mouse models, as
384 evidenced by the enhanced expression of relevant genes *Tgfbr1*, *Ctgf*, and *Pmepa1*,
385 leading to HSC activation (upregulated *Acta2*), and fibrosis progression (upregulated
386 *Fsp1*, *Actn1*, *Col1a1*, *Col1a2*, *Col3a1*) **(Figure 6A-E)**. Moreover, immunoblotting and
387 IF/IHC staining further confirmed suppression of EGFR activation, downregulation of
388 Ecm1 expression, and activation of Nrf2 signals in liver tissue of mice treated for 6-

389 weeks with CCl_4 **(Figure 6F, G; Suppl. Fig. 10)** or fed a Western diet (WD) for 12-
390 weeks **(Figure 6H, I)**, both supporting our findings in CLD models.

391 **Overexpression of ECM1 inhibits WD-induced liver injuries**

392 MASLD is the most common liver disease, with its severe form, MASH, characterized
393 by liver inflammation and fibrosis, which can progress to cirrhosis and HCC (Wang *et*
394 *al*, 2024). Lipid droplets that accumulate during the progression of MASLD change the
395 composition of free fatty acids, triglycerides, cholesterol, and phospholipids, thereby
396 inducing oxidative stress in the liver (Wang *et al.*, 2024). Since we found the activation
397 of IFNγ/ROS signaling and downregulation of EGFR/ECM1 in mouse models fed with
398 HFD/WD, we investigated whether ECM1 overexpression prevents WD-induced liver
399 fibrosis. Therefore, we treated 8-week-old WT mice with control or AAV8-ECM1 for
400 7 days prior to 12 weeks of WD feeding (Chow diet (CD) was used as control) **(Figure**
401 **6J)**. WD treatment resulted in significant activation of latent TGF-β1 (LTGF-β1), as
402 evidenced by the increased expression of LAP-D R58, a breakdown product of the
403 TGF-β1 LAP deposited in the ECM upon LTGF-β1 activation (**Figure 6K**).
404 Additionally, WD-fed mice showed upregulation of HSC-specific fibrosis markers,
405 including α-SMA and Col1a1 (**Figures 6L, M**), and exhibited moderate hepatic fibrosis
406 and liver injury, confirmed by PSR and H&E staining (**Figure 6N**). Remarkably, all
407 these pathological changes were significantly attenuated by AAV8-ECM1 treatment
408 (**Figures 6K-O**). Successful ECM1 overexpression was confirmed via IF staining
409 (**Figure 6L**). Interestingly, AAV8-ECM1 also appeared to reduce fat accumulation in
410 the liver tissue of WD-treated mice, as indicated by the lipid droplets of the white
411 bubbles in the H&E staining (**Figure 6N, O**). However, whether this effect is mediated
412 through TGF-β signaling or alternative pathways warrants further investigation. Taken
413 together, ECM1 overexpression effectively prevents liver fibrosis and injuries induced
414 by WD treatment, suggesting its potential benefit in MASLD progression.

415 **Inhibited EGFR, activated IFNγ/NRF2, and decreased ECM1 expression**
416 **aggravate the progression of fibrotic liver diseases**
417 To further verify the relevance of reduced ECM1 expression and its link to inhibited
418 EGF signaling, activated NRF2, and enhanced TGF-β signaling in CLD patients, we
419 performed IF or IHC staining for ECM1, EGFR, NRF2, and TGF-β1 LAP-D R58 in
420 the liver tissue from patients with early stages of liver fibrosis (F1-F2 fibrosis) or more
421 severe disease stages of F3-F4 fibrosis. The expression of ECM1 and EGFR decreased
422 at the F3-F4 stage compared to F1-F2 patients, whereas nuclear NRF2 and latent TGF-
423 β activation (LAP-D R58) increased considerably with disease progression **(Figure**
424 **7A)**. Quantification of the stainings implicated a positive correlation between the
425 expression of EGFR and ECM1 (correlation coefficient 0.9710) **(Figure 7B),** whereas
426 there is a negative correlation between NRF2 and ECM1 (correlation coefficient -
427 0.835) **(Figure 7C)**. This was further confirmed by analysing the GEO dataset
428 GSE49541 (Moylan *et al*, 2014; Murphy *et al*, 2013) that comprises mRNA expression
429 data of liver tissue from MASLD patients with mild (n=40) or advanced (n=32) fibrosis.
430 Gene set variation analyses (GSVA) revealed significant activation and upregulation of
431 IFNγ-, NRF2-, and TGF-β-related pathways in patients with advanced liver fibrosis,
432 including, among others, the oxidative stress pathway, the TGF-β signaling pathway,
433 the inflammatory response, type II interferon signaling, and the NRF2 pathway **(Figure**
434 **7D)**. We further analyzed the expression of key genes involved in these pathways,
435 which showed that the mRNA expression of *IFNGR1*, *STAT1,* and *NFE2L2* target
436 genes, including *CYP1B1* and *NQO1*, did increase with disease severity, while mRNA
437 levels of *ECM1* were decreased, leading to enhanced TGF-β signaling (*TGFBR1,*
438 *SMAD2, CTGF, PMEPA1*) (Link *et al.*, 2024), supported by the presence of upregulated
439 HSC activation marker *ACTA2* (encoding α-SMA) and fibrogenic gene expression,
440 including collagens, such as *FSP1*, *ACTN1*, *COL1A1*, *COL1A2*, and *COL3A1* in the
441 patients with more advanced fibrosis **(Figure 7E)**. Moreover, scRNA-seq dataset
442 GSE174748 including two normal liver samples and two MASLD cirrhotic liver

443 samples was analyzed (Filliol *et al.*, 2022). Unsupervised clustering classified cells into
444 14 different clusters **(Suppl. Fig. 11A)**. Based on the marker genes illustrated in **Suppl.**
445 **Fig. 11B**, we were able to classify the cell clusters into various categories including B
446 cell, Macrophage, T cell, Choloangiocyte, Endothelial cell, HSC and Hepatocyte
447 **(Figure 7F)**. Differential expression analysis in the hepatocytes between healthy and
448 cirrhotic livers was performed **(Figure 7G)**. Heatmap showed that in the hepatocytes
449 of cirrhotic livers, the expression of *ECM1*, *EGFR* were significantly deseased whereas
450 *IFNGR1* and the downstream targets of NRF2, *CYP1B1* and *NQO1*, were dramatically
451 increased. Additionally, the enhancement of TGF-β signaling was evidenced by
452 upregulated expression of *TGFBR1* in the hepatocytes from cirrhotic livers **(Figure 7H)**.
453 Similar results were also confirmed in MASLD/MASH patients from the
454 aforementioned dataset GSE202379 (Gribben *et al.*, 2024), where downregulation of
455 *ECM1* was accompanied by upregulation of *IFNGR1*, *NFE2L2* and *TGFBR1*, as well
456 as *COL1A1*, compared to healthy donors **(Figure 7I)**.
457 In conclusion, (1) in healthy hepatocytes, the EGF/EGFR/STAT1 signaling pathway
458 maintains ECM1 expression. However, (2) upon liver injury, IFNγ accumulates in the
459 liver and abrogates the expression of ECM1 through blocking EGFR expression and
460 (3) promoting NRF2 nuclear translocation, which binds to and negatively regulates the
461 *ECM1* gene promoter **(Figure 7J)**, leading to ECM1 downregulation, LTGF-β
462 activation, and CLD progression. The regulatory mechanism of ECM1 is further
463 validated in various CLD mouse models treated with CCl_4, BDL, *Fxr*-KO, DDC diet,
464 or CD-HFD. Moreover, ECM1 overexpression effectively attenuates MASLD
465 progression induced by WD treatment.

466 **Discussion**

467 This study investigated the regulation of ECM1 expression in hepatocytes under
468 various pathophysiological conditions associated with liver disease. Given hepatocytes
469 are the most vulnerable cells in the liver (Gribben *et al.*, 2024), ECM1 expression is

470 rapidly and significantly decreased in hepatocytes following injury. Although HSCs
471 also secrete ECM1, which serves as an important marker for their quiescence, the
472 reduction of ECM1 by activated HSCs occurs subsequent to hepatocyte injury (Fan *et*
473 *al.*, 2019; Link *et al.*, 2024). This suggests that the downregulation of ECM1 in injured
474 hepatocytes during the early stages of CLD may be a key factor in driving fibrosis
475 progression. Nevertheless, we examined the effects of EGF, IFNγ, and OPZ on *ECM1*
476 expression in human HSC LX-2 cells. However, these factors did not significantly
477 affect *ECM1* expression, indicating that the regulation of ECM1 in HSCs differs from
478 that in hepatocytes and warrants further investigation.
479 Our results showed that EGF promotes, whereas IFNγ inhibits ECM1 expression. Why
480 is the regulation of ECM1 expression so different despite the fact they both exploit
481 STAT1 signaling? Based on three lines of evidence, we elucidated that IFNγ and EGF-
482 induced STAT1 Ser727 phosphorylation are mechanistically independent events: (1)
483 Tyr701 phosphorylation of STAT1 is necessary for IFNγ-induced STAT1 Ser727
484 phosphorylation (Sadzak *et al.*, 2008). However, Ser727 phosphorylation induced by
485 the p38 mitogen-activated protein kinase (MAPK) is independent of Tyr701
486 phosphorylation (Kovarik *et al*, 1999). (2) EGF induced Ser727 phosphorylation alone
487 without Tyr701 phosphorylation (Zhang *et al.*, 2004), which is consistent with our
488 results **(Figure 3B)**. (3) EGF treatment enhanced STAT1 binding to the *Ecm1* promoter
489 **(Figure 2H, I; Suppl. Fig. 7B, C)**, whereas IFNγ treatment impeded the EGF-
490 promoted binding **(Figure 3C, D)**. It is important to recognize the multipotent effects
491 of STAT1 signaling, which may be regulated by EGF and involve essential
492 physiological functions beyond IFNγ. In mammary carcinoma cells, EGF/STAT1
493 signaling can antagonize the growth-inhibitory effects of TGF-β signaling via EGFR-
494 AKT-mediated phosphorylation of Smad3 at S208 (Huang *et al*, 2018). Conversely,
495 TGF-β signaling can affect the EGF/STAT1 pathway by downregulating EGFR
496 expression, therewith inhibiting STAT1 activation and reducing its DNA binding ability
497 (Baba *et al*, 2022; Huang *et al.*, 2018). We now add the knowledge that, in the liver,

498 EGF/STAT1 can inhibit latent TGF-β activation through ECM1 expression
499 upregulation.
500 IFNγ, mainly produced by activated T cells and natural killer cells, is an anti-viral, pro-
501 inflammatory and anti-tumorigenic cytokine, and has been reported to have anti-fibrotic
502 properties in hepatic fibrosis associated with chronic HBV infections (Weng *et al*,
503 2005). One trial showed that nine-month IFNγ treatment improves fibrosis scores in
504 patients through antagonizing TGF-β signaling (Weng *et al.*, 2005). *In vitro*, IFNγ
505 inhibits the proliferation and activation of HSCs, thereby inhibiting liver fibrosis (Jeong
506 *et al*, 2006; Weng *et al.*, 2007). Nonetheless, IFNγ also induces hepatocyte apoptosis
507 (Tagawa *et al*, 1997), hepatic inflammation, and inhibits hepatocyte proliferation, liver
508 regeneration (Sun *et al*, 2006), contributing to liver fibrogenesis. In viral hepatitis, the
509 hepatic lesions can be attributed to T cell-dependent cytotoxicity against virus-infected
510 hepatocytes, where IFNγ, which is typically elevated in patients with chronic viral liver
511 disease (Fukuda *et al*, 1995), plays a crucial role. When IFNγ was administered to HBV
512 transgenic mice that did not develop hepatitis, hepatic lesions with lymphocytes
513 infiltration were observed (Gilles *et al*, 1992). Moreover, in a methionine and choline-
514 deficient high-fat (MCDHF) diet mouse model, IFNγ was even identified as a pro-
515 fibrotic cytokine (Luo *et al*, 2013). NRF2 is activated by inflammatory mediators such
516 as ROS, fatty acids, nitric oxide and prostaglandins (Saha *et al*, 2020), which is
517 considered to provide a cytoprotective effect. However, excessive activation of NRF2
518 and a consecutive nuclear accumulation has detrimental effects. In a *Keap1*-null mouse
519 model, no newborns survived after three weeks, possibly due to starvation caused by a
520 hyperkeratotic esophagus and cardia (Wakabayashi *et al*, 2003). Additionally, an
521 association between NRF2 and hepatic steatosis was identified, demonstrating that a
522 specific deletion of NRF2 in hepatocytes reduced the expression of HFD-induced
523 PPARγ and lipid accumulation, thus impairing the progression of MASLD (Li *et al*,
524 2020). Moreover, pancreatic cancer patients with elevated NRF2 levels have a shorter
525 median survival time (Su *et al*, 2022). Our findings suggest that both, NRF2 and IFNγ

526 integrate in damage stressed hepatocytes towards, among others, downregulation of
527 ECM1. Loss of ECM1 is a kind of negative damage-associated molecular pattern
528 (DAMP) reaction, which results in extracellular decrease in ECM1 availability,
529 subsequent LTGF-β activation. Thus, increased amounts of active TGF-β now can
530 activate HSCs and induce fibrogenesis. In terms of anti-fibrotic therapy, while using
531 IFNγ to inhibit HSC activation or NRF2 agonist in CLD patients, their potential adverse
532 effects on hepatocytes should also be considered.
533 Overall, the current study highlights the roles of EGF and IFNγ in regulating ECM1
534 expression in hepatocytes under physiological and pathological conditions. For the
535 clinical applicability of IFNγ and NRF2 agonist, the potential hepatotoxicity resulting
536 from IFNγ and NRF2 over-accumulation should be carefully evaluated, as they
537 significantly inhibit ECM1 expression in hepatocytes. ECM1 has the potential to be
538 developed as an anti-fibrotic agent, especially in combination with IFNγ and NRF2
539 agonist. It will be interesting to further investigate whether ECM1-derived therapies
540 constitute an effective treatment route for CLD.

541 **Materials and Methods**

542 Human samples, mouse experiments, primers, and reagents used in this study, as well
543 as methodological details can be found in the supplementary materials.
544 This study includes no data deposited in external repositories.

545 **Acknowledgements**

546 We acknowledge the support of the LIMa Live Cell Imaging at Microscopy Core
547 Facility Platform Mannheim (CFPM).

548 **Declaration of interests**

549 The authors declare no competing interests.

550 **Abbreviations:**

ADAMTS1	A disintegrin and metalloproteinase with thrombospondin motifs 1
BDL	Bile duct ligation
BW	Body weight
CCl_4	Carbon tetrachloride
CD	Chow diet
CD-HFD	Choline-deficient high-fat diet
ChIP	Chromatin immunoprecipitation
CLD	Chronic liver disease
CYP1B1	cytochrome P450 family 1 subfamily B member 1
DDC	3,5-diethoxycarbonyl-1,4-dihydrocollidine
ECM1	Extracellular matrix protein 1
EGF	Epidermal growth factor
EGFR	Epidermal growth factor receptor
GEO	Gene Expression Omnibus
H_2O_2	Hydrogen peroxide
HBV	Hepatitis-B-virus
HCC	Hepatocellular carcinoma
HPHs	Human primary hepatocytes
HSCs	Hepatic stellate cells
IF	Immunofluorescence
IFNγ	Interferon gamma
IHC	Immunohistochemistry
i.p.	Intraperitoneal
KEAP1	Kelch-like ECH-associated protein 1
LAP	Latency-associated peptide
LTGF-β	Latent TGF-β
MELD	Model for End-Stage Liver Disease
MMP	Matrix metalloproteinase
MPHs	Mouse primary hepatocytes
MASLD	Metabolic dysfunction-associated steatotic liver disease
MASH	Metabolic dysfunction-associated steatohepatitis
NQO1	NAD(P)H:quinone oxidoreductase 1

NRF2	Nuclear factor erythroid 2-related factor 2
OPZ	Oltipraz
PSR	Picrosirius Red
qRT-PCR	Quantitative real-time PCR
ROS	Reactive oxygen species
scRNA-seq	single-cell RNA sequencing
siRNA	Small interfering RNA
S727	Serine727
TSP-1	Thrombospondin 1
TSS	Transcription start site
UMAP	Uniform manifold approximation and projection
WD	Western diet
Y701	Tyrosine701

551 **References**

552 ***Author names in bold designate shared co-first authorship***

553 Baba AB, Rah B, Bhat GR, Mushtaq I, Parveen S, Hassan R, Hameed Zargar M, Afroze D
554 (2022) Transforming Growth Factor-Beta (TGF-beta) Signaling in Cancer-A Betrayal
555 Within. *Front Pharmacol* 13: 791272

556 **Bai KH, He SY,** Shu LL, Wang WD, Lin SY, Zhang QY, Li L, Cheng L, Dai YJ (2020)
557 Identification of cancer stem cell characteristics in liver hepatocellular carcinoma by
558 WGCNA analysis of transcriptome stemness index. *Cancer Med* 9: 4290-4298

559 **Fan W, Liu T, Chen W,** Hammad S, Longerich T, Hausser I, Fu Y, Li N, He Y, Liu C *et al*
560 (2019) ECM1 Prevents Activation of Transforming Growth Factor beta, Hepatic Stellate
561 Cells, and Fibrogenesis in Mice. *Gastroenterology* 157: 1352-1367 e1313

562 Filliol A, Saito Y, Nair A, Dapito DH, Yu LX, Ravichandra A, Bhattacharjee S, Affo S,
563 Fujiwara N, Su H *et al* (2022) Opposing roles of hepatic stellate cell subpopulations in
564 hepatocarcinogenesis. *Nature* 610: 356-365

565 Fukuda R, Ishimura N, Nguyen TX, Chowdhury A, Ishihara S, Kohge N, Akagi S,
566 Watanabe M, Fukumoto S (1995) The expression of IL-2, IL-4 and interferon-gamma
567 (IFN-gamma) mRNA using liver biopsies at different phases of acute exacerbation of
568 chronic hepatitis B. *Clin Exp Immunol* 100: 446-451

569 **Gao F, Xia Y,** Wang J, Lin Z, Ou Y, Liu X, Liu W, Zhou B, Luo H, Zhou B *et al* (2014)
570 Integrated analyses of DNA methylation and hydroxymethylation reveal tumor
571 suppressive roles of ECM1, ATF5, and EOMES in human hepatocellular carcinoma.
572 *Genome Biol* 15: 533

573 Gilles PN, Guerrette DL, Ulevitch RJ, Schreiber RD, Chisari FV (1992) HBsAg retention
574 sensitizes the hepatocyte to injury by physiological concentrations of interferon-
575 gamma. *Hepatology* 16: 655-663

576 **Gribben C, Galanakis V,** Calderwood A, Williams EC, Chazarra-Gil R, Larraz M, Frau C,
577 Puengel T, Guillot A, Rouhani FJ *et al* (2024) Acquisition of epithelial plasticity in human
578 chronic liver disease. *Nature* 630: 166-173

579 **Hammad S, Ogris C,** Othman A, Erdoesi P, Schmidt-Heck W, Biermayer I, Helm B, Gao
580 Y, Pioronska W, Holland CH *et al* (2023) Tolerance of repeated toxic injuries of murine
581 livers is associated with steatosis and inflammation. *Cell Death Dis* 14: 414

582 **He F, Antonucci L, Yamachika S,** Zhang Z, Taniguchi K, Umemura A, Hatzivassiliou G,
583 Roose-Girma M, Reina-Campos M, Duran A *et al* (2020) NRF2 activates growth factor
584 genes and downstream AKT signaling to induce mouse and human hepatomegaly. *J*
585 *Hepatol* 72: 1182-1195

586 Holland CH, Ramirez Flores RO, Myllys M, Hassan R, Edlund K, Hofmann U, Marchan R,
587 Cadenas C, Reinders J, Hoehme S *et al* (2022) Transcriptomic Cross-Species Analysis of
588 Chronic Liver Disease Reveals Consistent Regulation Between Humans and Mice.
589 *Hepatol Commun* 6: 161-177

590 Horras CJ, Lamb CL, Mitchell KA (2011) Regulation of hepatocyte fate by interferon-
591 gamma. *Cytokine Growth Factor Rev* 22: 35-43

592 Huang F, Shi Q, Li Y, Xu L, Xu C, Chen F, Wang H, Liao H, Chang Z, Liu F *et al* (2018)
593 HER2/EGFR-AKT Signaling Switches TGFbeta from Inhibiting Cell Proliferation to
594 Promoting Cell Migration in Breast Cancer. *Cancer Res* 78: 6073-6085
595 Ijssennagger N, Janssen AWF, Milona A, Ramos Pittol JM, Hollman DAA, Mokry M,
596 Betzel B, Berends FJ, Janssen IM, van Mil SWC *et al* (2016) Gene expression profiling in
597 human precision cut liver slices in response to the FXR agonist obeticholic acid. *J*
598 *Hepatol* 64: 1158-1166
599 Jaeschke H, Woolbright BL (2012) Current strategies to minimize hepatic ischemia-
600 reperfusion injury by targeting reactive oxygen species. *Transplant Rev (Orlando)* 26:
601 103-114
602 Jeong WI, Park O, Radaeva S, Gao B (2006) STAT1 inhibits liver fibrosis in mice by
603 inhibiting stellate cell proliferation and stimulating NK cell cytotoxicity. *Hepatology* 44:
604 1441-1451
605 Kovarik P, Stoiber D, Eyers PA, Menghini R, Neininger A, Gaestel M, Cohen P, Decker T
606 (1999) Stress-induced phosphorylation of STAT1 at Ser727 requires p38 mitogen-
607 activated protein kinase whereas IFN-gamma uses a different signaling pathway. *Proc*
608 *Natl Acad Sci U S A* 96: 13956-13961
609 **Lee HJ, Oh YK,** Rhee M, Lim JY, Hwang JY, Park YS, Kwon Y, Choi KH, Jo I, Park SI *et al*
610 (2007) The role of STAT1/IRF-1 on synergistic ROS production and loss of mitochondrial
611 transmembrane potential during hepatic cell death induced by LPS/d-GalN. *J Mol Biol*
612 369: 967-984
613 **Li L, Cui L, Lin P,** Liu Z, Bao S, Ma X, Nan H, Zhu W, Cen J, Mao Y *et al* (2023) Kupffer-
614 cell-derived IL-6 is repurposed for hepatocyte dedifferentiation via activating
615 progenitor genes from injury-specific enhancers. *Cell Stem Cell* 30: 283-299 e289
616 **Li L, Fu J,** Liu D, Sun J, Hou Y, Chen C, Shao J, Wang L, Wang X, Zhao R *et al* (2020)
617 Hepatocyte-specific Nrf2 deficiency mitigates high-fat diet-induced hepatic steatosis:
618 Involvement of reduced PPARgamma expression. *Redox Biol* 30: 101412
619 Li Y, Fan W, Link F, Wang S, Dooley S (2022) Transforming growth factor beta latency: A
620 mechanism of cytokine storage and signalling regulation in liver homeostasis and
621 disease. *JHEP Rep* 4: 100397
622 Link F, Li Y, Zhao J, Munker S, Fan W, Nwosu ZC, Yao Y, Wang S, Huang C, Liebe R *et al*
623 (2024) ECM1 attenuates hepatic fibrosis by interfering with mediators of latent TGF-
624 beta1 activation. *Gut*
625 Luo XY, Takahara T, Kawai K, Fujino M, Sugiyama T, Tsuneyama K, Tsukada K, Nakae S,
626 Zhong L, Li XK (2013) IFN-gamma deficiency attenuates hepatic inflammation and
627 fibrosis in a steatohepatitis model induced by a methionine- and choline-deficient
628 high-fat diet. *Am J Physiol Gastrointest Liver Physiol* 305: G891-899
629 Mathieu E, Meheus L, Raymackers J, Merregaert J (1994) Characterization of the
630 osteogenic stromal cell line MN7: identification of secreted MN7 proteins using two-
631 dimensional polyacrylamide gel electrophoresis, western blotting, and
632 microsequencing. *J Bone Miner Res* 9: 903-913

633 Miyawaki A, Iizuka Y, Sugino H, Watanabe Y (2019) IL-11 prevents IFN-gamma-induced
634 hepatocyte death through selective downregulation of IFN-gamma/STAT1 signaling
635 and ROS scavenging. *PLoS One* 14: e0211123
636 Moylan CA, Pang H, Dellinger A, Suzuki A, Garrett ME, Guy CD, Murphy SK, Ashley-Koch
637 AE, Choi SS, Michelotti GA *et al* (2014) Hepatic gene expression profiles differentiate
638 presymptomatic patients with mild versus severe nonalcoholic fatty liver disease.
639 *Hepatology* 59: 471-482
640 Murphy SK, Yang H, Moylan CA, Pang H, Dellinger A, Abdelmalek MF, Garrett ME,
641 Ashley-Koch A, Suzuki A, Tillmann HL *et al* (2013) Relationship between methylome
642 and transcriptome in patients with nonalcoholic fatty liver disease. *Gastroenterology*
643 145: 1076-1087
644 Platanias LC (2005) Mechanisms of type-I- and type-II-interferon-mediated signalling.
645 *Nat Rev Immunol* 5: 375-386
646 Sadzak I, Schiff M, Gattermeier I, Glinitzer R, Sauer I, Saalmuller A, Yang E, Schaljo B,
647 Kovarik P (2008) Recruitment of Stat1 to chromatin is required for interferon-induced
648 serine phosphorylation of Stat1 transactivation domain. *Proc Natl Acad Sci U S A* 105:
649 8944-8949
650 Saha S, Buttari B, Panieri E, Profumo E, Saso L (2020) An Overview of Nrf2 Signaling
651 Pathway and Its Role in Inflammation. *Molecules* 25
652 Sercu S, Lambeir AM, Steenackers E, El Ghalbzouri A, Geentjens K, Sasaki T, Oyama N,
653 Merregaert J (2009) ECM1 interacts with fibulin-3 and the beta 3 chain of laminin 332
654 through its serum albumin subdomain-like 2 domain. *Matrix Biol* 28: 160-169
655 Sercu S, Zhang L, Merregaert J (2008) The extracellular matrix protein 1: its molecular
656 interaction and implication in tumor progression. *Cancer Invest* 26: 375-384
657 Smits P, Poumay Y, Karperien M, Tylzanowski P, Wauters J, Huylebroeck D, Ponec M,
658 Merregaert J (2000) Differentiation-dependent alternative splicing and expression of
659 the extracellular matrix protein 1 gene in human keratinocytes. *J Invest Dermatol* 114:
660 718-724
661 **Su H, Yang F,** Fu R, Trinh B, Sun N, Liu J, Kumar A, Baglieri J, Siruno J, Le M *et al* (2022)
662 Collagenolysis-dependent DDR1 signalling dictates pancreatic cancer outcome. *Nature*
663 610: 366-372
664 Sun R, Park O, Horiguchi N, Kulkarni S, Jeong WI, Sun HY, Radaeva S, Gao B (2006) STAT1
665 contributes to dsRNA inhibition of liver regeneration after partial hepatectomy in mice.
666 *Hepatology* 44: 955-966
667 **Suppli MP, Rigbolt KTG,** Veidal SS, Heeboll S, Eriksen PL, Demant M, Bagger JI, Nielsen
668 JC, Oro D, Thrane SW *et al* (2019) Hepatic transcriptome signatures in patients with
669 varying degrees of nonalcoholic fatty liver disease compared with healthy normal-
670 weight individuals. *Am J Physiol Gastrointest Liver Physiol* 316: G462-G472
671 Tagawa Y, Sekikawa K, Iwakura Y (1997) Suppression of concanavalin A-induced
672 hepatitis in IFN-gamma(-/-) mice, but not in TNF-alpha(-/-) mice: role for IFN-gamma
673 in activating apoptosis of hepatocytes. *J Immunol* 159: 1418-1428

674 **Trepo E, Goossens N,** Fujiwara N, Song WM, Colaprico A, Marot A, Spahr L, Demetter
675 P, Sempoux C, Im GY *et al* (2018) Combination of Gene Expression Signature and Model
676 for End-Stage Liver Disease Score Predicts Survival of Patients With Severe Alcoholic
677 Hepatitis. *Gastroenterology* 154: 965-975
678 Wakabayashi N, Itoh K, Wakabayashi J, Motohashi H, Noda S, Takahashi S, Imakado S,
679 Kotsuji T, Otsuka F, Roop DR *et al* (2003) Keap1-null mutation leads to postnatal
680 lethality due to constitutive Nrf2 activation. *Nat Genet* 35: 238-245
681 Wang L, Yu J, Ni J, Xu XM, Wang J, Ning H, Pei XF, Chen J, Yang S, Underhill CB *et al*
682 (2003) Extracellular matrix protein 1 (ECM1) is over-expressed in malignant epithelial
683 tumors. *Cancer Lett* 200: 57-67
684 Wang S, Link F, Han M, Chaudhary R, Asimakopoulos A, Liebe R, Yao Y, Hammad S,
685 Dropmann A, Krizanac M *et al* (2024) The Interplay of TGF-beta1 and Cholesterol
686 Orchestrating Hepatocyte Cell Fate, EMT, and Signals for HSC Activation. *Cell Mol*
687 *Gastroenterol Hepatol* 17: 567-587
688 Wang Z (2017) ErbB Receptors and Cancer. *Methods Mol Biol* 1652: 3-35
689 Weng H, Mertens PR, Gressner AM, Dooley S (2007) IFN-gamma abrogates
690 profibrogenic TGF-beta signaling in liver by targeting expression of inhibitory and
691 receptor Smads. *J Hepatol* 46: 295-303
692 Weng HL, Wang BE, Jia JD, Wu WF, Xian JZ, Mertens PR, Cai WM, Dooley S (2005) Effect
693 of interferon-gamma on hepatic fibrosis in chronic hepatitis B virus infection: a
694 randomized controlled study. *Clin Gastroenterol Hepatol* 3: 819-828
695 **Yoo S, Wang W, Wang Q,** Fiel MI, Lee E, Hiotis SP, Zhu J (2017) A pilot systematic
696 genomic comparison of recurrence risks of hepatitis B virus-associated hepatocellular
697 carcinoma with low- and high-degree liver fibrosis. *BMC Med* 15: 214
698 Zeineldin R, Hudson LG (2006) Epithelial cell migration in response to epidermal
699 growth factor. *Methods Mol Biol* 327: 147-158
700 Zhang Y, Cho YY, Petersen BL, Zhu F, Dong Z (2004) Evidence of STAT1 phosphorylation
701 modulated by MAPKs, MEK1 and MSK1. *Carcinogenesis* 25: 1165-1175

Figure and figure legend

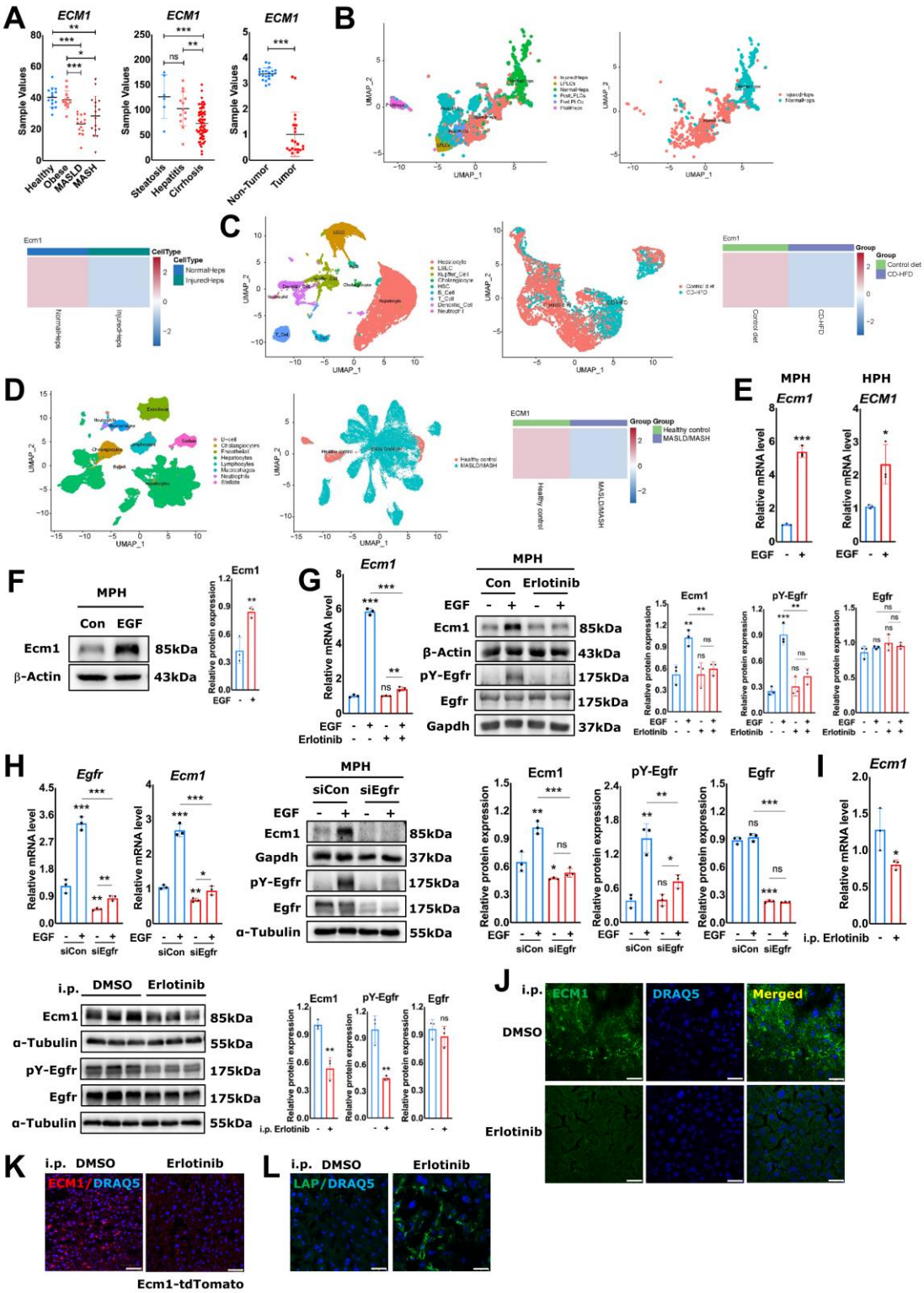

Figure 1. EGF-EGFR signaling maintains Ecm1 expression in hepatocytes of quiescent liver

(A) mRNA expression of hepatic *ECM1* in CLD patients, extracted from the GEO Dataset GSE126848, GSE103580 and GSE94660, respectively. UMAP visualization of cell populations and hepatocytes, and heatmap of *ECM1* mRNA expression in **(B)** DDC mouse model (GSE193850), **(C)** CD-HFD fed mice (GSE232182), and **(D)** patients with CLD (GSE202379). **(E)** qRT-PCR for *ECM1* mRNA expression in MPHs and HPHs with or without EGF treatment. **(F)** Immunoblotting of Ecm1 in MPHs treated with EGF. **(G)** qRT-PCR and immunoblotting showing the effect of erlotinib on Ecm1 expression and Egfr Y1068 phosphorylation in MPHs with or without EGF treatment. **(H)** Effects of *Egfr* knockdown on mRNA and protein expression of Ecm1 and Egfr in EGF-treated MPHs by qRT-PCR and immunoblotting. **(I)** qRT-PCR and immunoblotting for Ecm1 in liver tissues from DMSO or erlotinib-treated mice. DMSO was administered as a placebo. **(J)** Representative IF staining for Ecm1 expression in liver tissues from DMSO or erlotinib-treated mice. DRAQ5 fluorescent probe stains DNA. **(K)** Representative tdTomato fluorescence of liver tissues from Ecm1-tdTomato mice treated with DMSO or erlotinib. **(L)** Representative IF staining for LAP-D R58 in liver tissues from DMSO or erlotinib-treated mice. Scale bar, 25μm. The results of qRT-PCR were normalized to *PPIA*. In immunoblotting, β-Actin, Gapdh and α-Tubulin are loading controls. Quantification of protein expression was performed by ImageJ (National Institutes of Health, Bethesda, Maryland, USA). *P*-values were calculated by unpaired Student's t test. Bars represent the mean ± SD. *, $P<0.05$; **, $P<0.01$; ***, $P<0.001$.

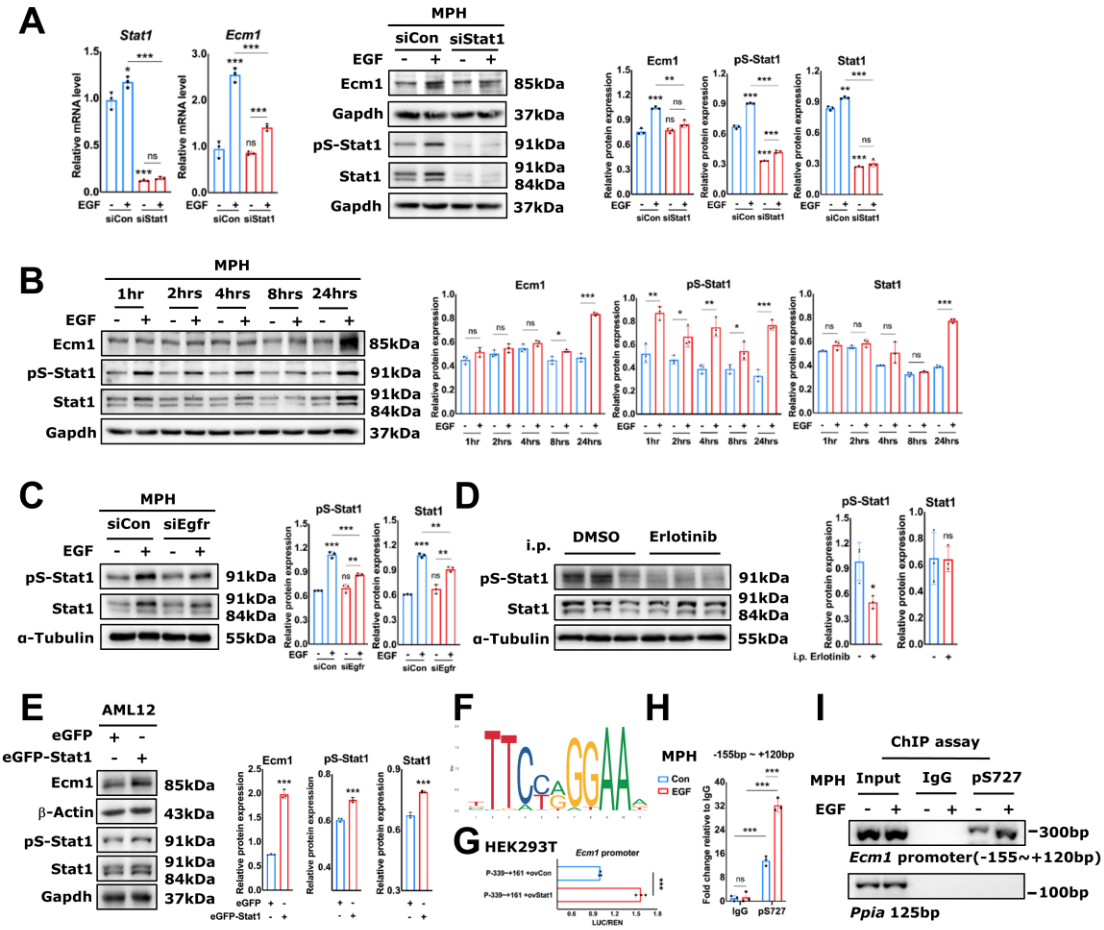
A
Stat1
Ecm1
Relative mRNA level
EGF
siCon siStat1
MPH
siCon siStat1
EGF
Ecm1
Gapdh
pS-Stat1
Stat1
Gapdh
85kDa
37kDa
91kDa
91kDa
84kDa
37kDa
Relative protein expression
B
MPH
1hr 2hrs 4hrs 8hrs 24hrs
EGF
Ecm1
pS-Stat1
Stat1
Gapdh
85kDa
91kDa
91kDa
84kDa
37kDa
C
MPH
siCon siEgfr
EGF
pS-Stat1
Stat1
α-Tubulin
91kDa
91kDa
84kDa
55kDa
D
i.p.
DMSO
Erlotinib
pS-Stat1
Stat1
α-Tubulin
91kDa
91kDa
84kDa
55kDa
i.p. Erlotinib
E
AML12
eGFP
eGFP-Stat1
Ecm1
β-Actin
pS-Stat1
Stat1
Gapdh
85kDa
43kDa
91kDa
91kDa
84kDa
37kDa
F
G
HEK293T
Ecm1 promoter
LUC/REN
H
MPH
-155bp ~ +120bp
Con
EGF
Fold change relative to IgG
IgG
pS727
I
ChIP assay
MPH
Input
IgG
pS727
EGF
-300bp
Ecm1 promoter(-155~+120bp)
-100bp
Ppia 125bp

725 **Figure 2. EGF regulates homeostatic Ecm1 expression in hepatocytes through**
726 **Stat1**
727 **(A)** qRT-PCR and immunoblotting of Ecm1 and Stat1 in EGF-treated MPHs with or
728 without *Stat1* knockdown. **(B)** Immunoblotting showing the effect of EGF on target
729 proteins in MPHs at different time points. **(C)** Immunoblotting for p-Stat1 S727 and
730 Stat1 in EGF-treated MPHs with or without knockdown *Egfr*. **(D)** Immunoblotting for
731 p-Stat1 S727 and Stat1 in liver tissue from DMSO or erlotinib-treated mice. DMSO
732 was administered as a placebo. **(E)** Immunoblotting for Ecm1, p-Stat1 S727 and total
733 Stat1 in AML12 cells transfected with expression vectors. **(F)** Predicted binding motif
734 of Stat1 to *Ecm1* promoter by Jaspar. **(G)** Luciferase reporter assay analyzing the
735 activity of *Ecm1* promoter (-339 ~ +161bp) in HEK293T cells transfected with or
736 without Stat1 plasmid. **(H)** ChIP qRT-PCR showing the binding of S727
737 phosphorylated Stat1 to the *Ecm1* gene promoter in MPHs, with or without EGF
738 treatment. Fragment "-155bp ~ +120bp" is calculated relative to the *Ecm1* gene TSS.
739 Rabbit IgG-bound chromatin served as negative control. **(I)** The amplified products of
740 ChIP PCR are shown as bands on 2% agarose gel. *Ppia* represents non-specific binding.
741 The results of qRT-PCR were normalized to *Ppia*. For immunoblotting, Gapdh, α-
742 Tubulin and β-Actin are loading controls. Figure C and D shared same loading controls
743 as Figure 1H and 1I. Quantification of protein expression was done by ImageJ (National
744 Institutes of Health, Bethesda, Maryland, USA). *P*-values were calculated by unpaired
745 Student's t test. Bars represent the mean ± SD. *, $P<0.05$; **, $P<0.01$; ***, $P<0.001$.

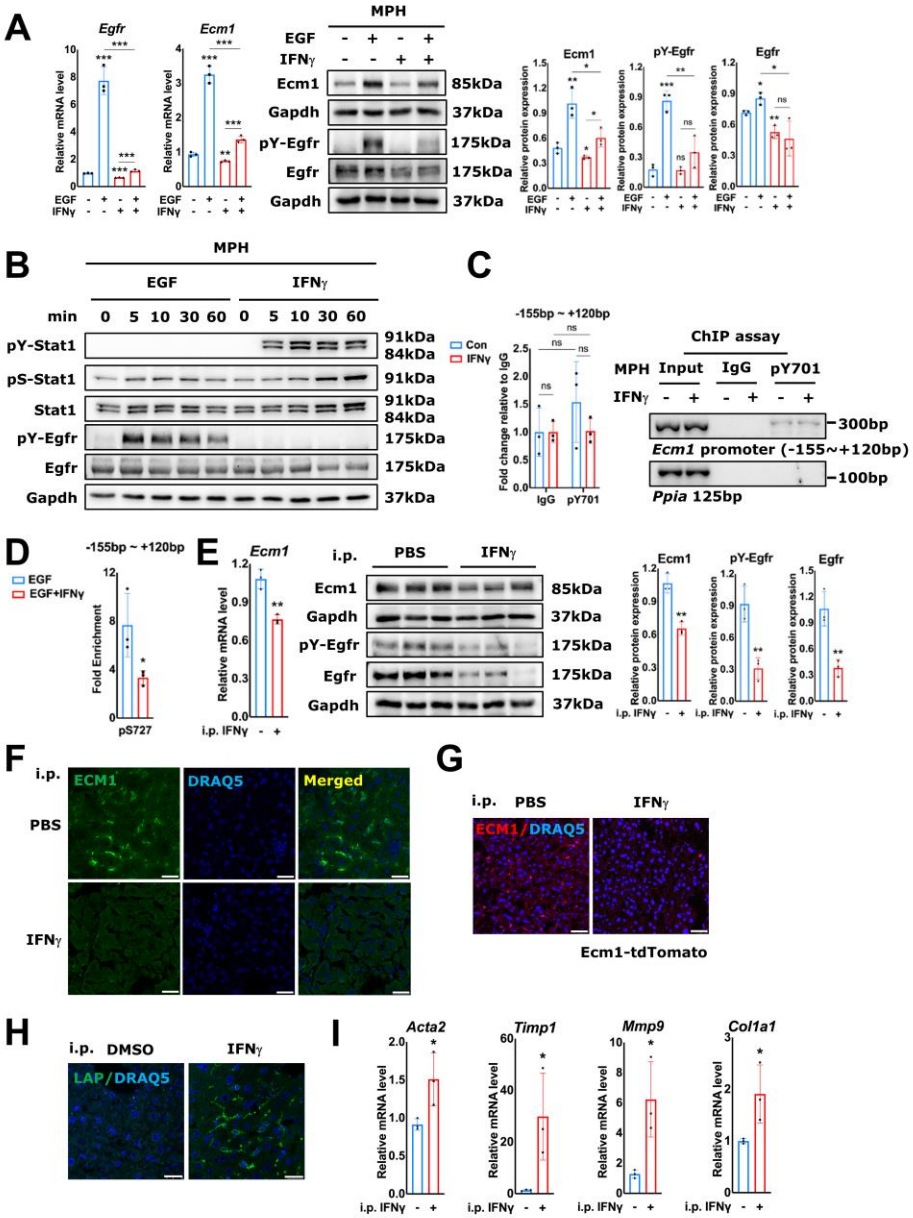
A
Egfr
Ecm1
Relative mRNA level
MPH
EGF
IFNγ
Ecm1
Gapdh
pY-Egfr
Egfr
85kDa
37kDa
175kDa
Relative protein expression
B
min
0 5 10 30 60 0 5 10 30 60
pY-Stat1
pS-Stat1
Stat1
91kDa
84kDa
Con
C
-155bp ~ +120bp
Fold change relative to IgG
IgG
pY701
ChIP assay
MPH Input IgG pY701
300bp
Ecm1 promoter (-155~+120bp)
100bp
Ppia 125bp
D
EGF
EGF+IFNγ
Fold Enrichment
pS727
E
i.p.
PBS
i.p. IFNγ
F
ECM1
DRAQ5
Merged
G
ECM1/DRAQ5
Ecm1-tdTomato
H
DMSO
LAP/DRAQ5
I
Acta2
Timp1
Mmp9
Col1a1

746 **Figure 3. IFNγ abrogates EGF-EGFR-maintained Ecm1 expression**

747 **(A)** qRT-PCR and immunoblotting showing the impact of IFNγ on Ecm1 and Egfr
748 expression in EGF-treated MPHs. **(B)** Immunoblotting showing the effect of EGF or
749 IFNγ on target proteins in MPHs at different time points. **(C)** ChIP qRT-PCR displaying
750 the effect of IFNγ treatment on the binding of p-Stat1 Y701 to the *Ecm1* gene promoter
751 in MPHs. ChIP PCR amplified products were separated on 2% agarose gel. The
752 fragment positions "-155bp ~ +120bp" are calculated relative to the *Ecm1* gene TSS.
753 Rabbit IgG-bound chromatin served as negative control. *Ppia* represents non-specific
754 binding. **(D)** Fold enrichment from ChIP qRT-PCR showing the effect of IFNγ
755 treatment on EGF-induced Stat1 binding to the *Ecm1* gene promoter in MPHs. **(E)** qRT-
756 PCR and immunoblotting showing target genes or proteins in liver tissue from PBS or
757 IFNγ-treated mice. PBS was administered as placebo. **(F)** Representative IF staining
758 for Ecm1 expression in the liver tissue from PBS or IFNγ-treated mice. DRAQ5
759 fluorescent probe stains DNA. **(G)** Representative tdTomato fluorescence of liver tissue
760 from Ecm1-tdTomato mice treated with PBS or IFNγ. **(H)** Representative IF staining
761 for LAP-D R58 in liver tissues from PBS or IFNγ-treated mice. **(I)** qRT-PCR showing
762 the impact of IFNγ on *Acta2*, *Timp1*, *Mmp9*, *Col1a1* expression in liver tissues from
763 IFNγ-treated mice. Scale bar, 25μm. The results of qRT-PCR are normalized to *Ppia*.
764 Gapdh was used as loading control. Quantification of protein expression was done by
765 ImageJ (National Institutes of Health, Bethesda, Maryland, USA). *P*-values were
766 calculated by unpaired Student's t test. Bars represent the mean ± SD. *, $P<0.05$; **,
767 $P<0.01$; ***, $P<0.001$.

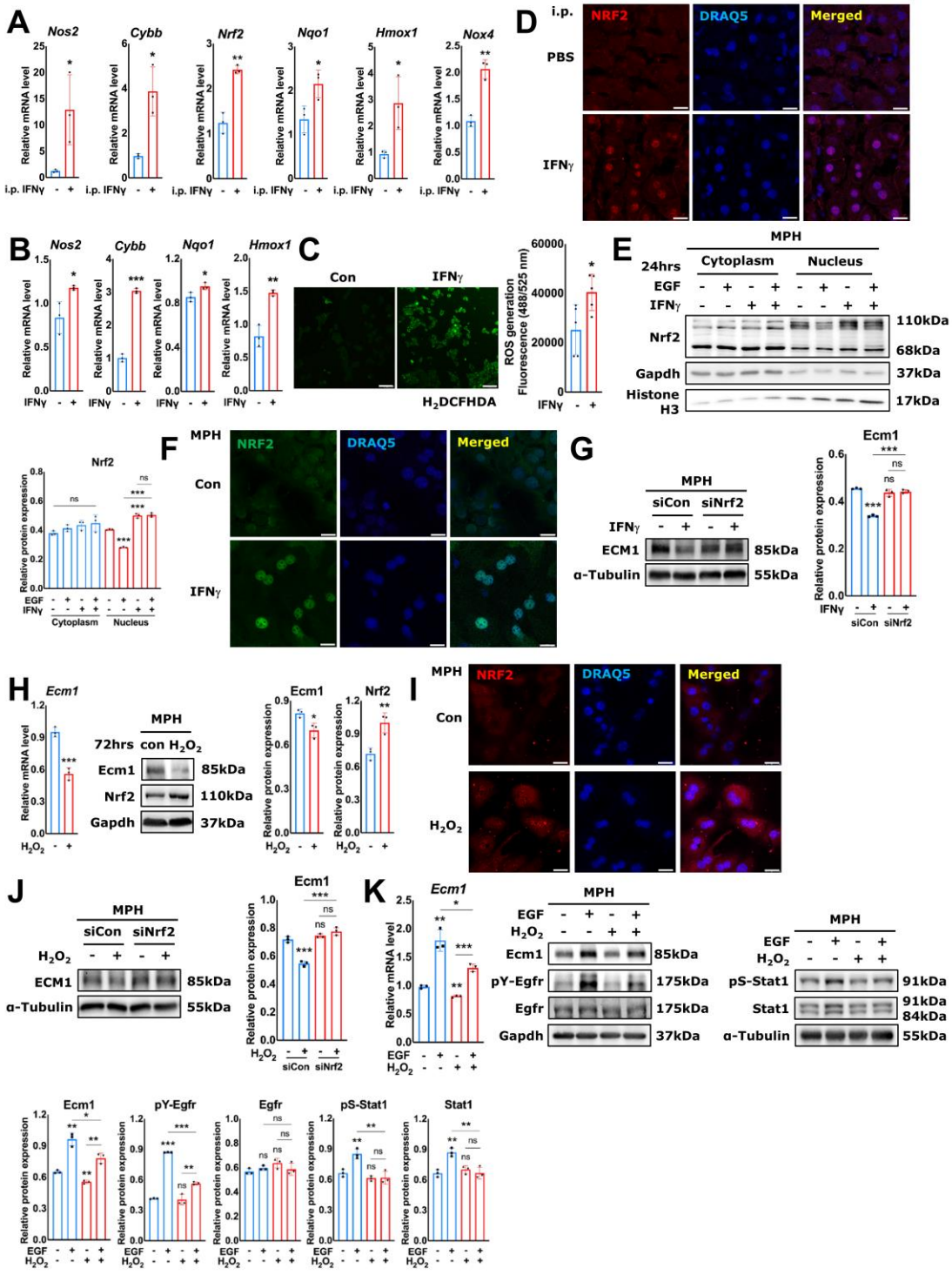
A
Nos2
Cybb
Nrf2
Nqo1
Hmox1
Nox4
Relative mRNA level
i.p. IFNγ - +
D
i.p.
NRF2
DRAQ5
Merged
PBS
IFNγ
B
Nos2
Cybb
Nqo1
Hmox1
Relative mRNA level
IFNγ - +
C
Con
IFNγ
H2DCFHDA
ROS generation Fluorescence (488/525 nm)
IFNγ - +
E
MPH
24hrs
Cytoplasm
Nucleus
EGF
IFNγ
Nrf2
110kDa
68kDa
Gapdh
37kDa
Histone H3
17kDa
Nrf2
Relative protein expression
EGF
IFNγ
Cytoplasm
Nucleus
F
MPH
NRF2
DRAQ5
Merged
Con
IFNγ
G
MPH
siCon
siNrf2
IFNγ
ECM1
85kDa
α-Tubulin
55kDa
Ecm1
Relative protein expression
IFNγ
siCon
siNrf2
H
Ecm1
Relative mRNA level
H2O2 - +
MPH
72hrs
con
H2O2
Ecm1
85kDa
Nrf2
110kDa
Gapdh
37kDa
Ecm1
Nrf2
Relative protein expression
H2O2 - +
I
MPH
NRF2
DRAQ5
Merged
Con
H2O2
J
MPH
siCon
siNrf2
H2O2
ECM1
85kDa
α-Tubulin
55kDa
Ecm1
Relative protein expression
H2O2
siCon
siNrf2
K
Ecm1
Relative mRNA level
EGF
H2O2
MPH
Ecm1
85kDa
pY-Egfr
175kDa
Egfr
175kDa
Gapdh
37kDa
pS-Stat1
91kDa
Stat1
91kDa
84kDa
α-Tubulin
55kDa
Ecm1
pY-Egfr
Egfr
pS-Stat1
Stat1
Relative protein expression
EGF
H2O2

768 **Figure 4. IFNγ inhibits Ecm1 expression through Nrf2**

769 **(A)** qRT-PCR for mRNA expression levels of *Nos2*, *Cybb*, *Nrf2*, *Nqo1*, *Hmox1* and
770 *Nox4* in liver tissues from IFNγ-treated mice. **(B)** qRT-PCR for mRNA expression
771 levels of *Nos2*, *Cybb*, *Nqo1*, *Hmox1* in IFNγ-treated MPHs. **(C)** ROS generation
772 fluorescence detection in the MPHs treated with IFNγ. **(D)** Representative IF staining
773 for Nrf2 expression in liver tissues from PBS or IFNγ-treated mice. Scale bar, 12.5μm.
774 **(E)** Immunoblotting for cytoplasmic and nuclear localization of Nrf2 in MPHs treated
775 with EGF and/or IFNγ. **(F)** Representative IF staining showing expression and
776 localization of Nrf2 in IFNγ-treated MPHs. Scale bar, 25μm. **(G)** Immunoblotting
777 showing the impact of *Nrf2* knockdown on Ecm1 expression in IFNγ-treated MPHs.
778 **(H)** qRT-PCR and immunoblotting showing the impact of H_2O_2 treatment on Ecm1 and
779 Nrf2 expression in MPHs. **(I)** Representative IF staining showing Nrf2 expression in
780 H_2O_2-treated MPHs. Scale bar, 25μm. **(J)** Immunoblotting showing the impact of
781 knockdown *Nrf2* on Ecm1 expression in H_2O_2-treated MPHs. **(K)** qRT-PCR and
782 immunoblotting showing the effect of H_2O_2 on target genes or proteins in EGF-treated
783 MPHs. The results of qRT-PCR are normalized to *Ppia*. Gapdh/α-Tubulin and Histone
784 H3 are loading controls for cytoplasmic and nuclear proteins, respectively. DRAQ5
785 fluorescent probe stains DNA. Quantification of protein expression was done by ImageJ
786 (National Institutes of Health, Bethesda, Maryland, USA). *P*-values were calculated by
787 unpaired Student's t test. Bars represent the mean ± SD. *, $P<0.05$; **, $P<0.01$; ***,
788 $P<0.001$.

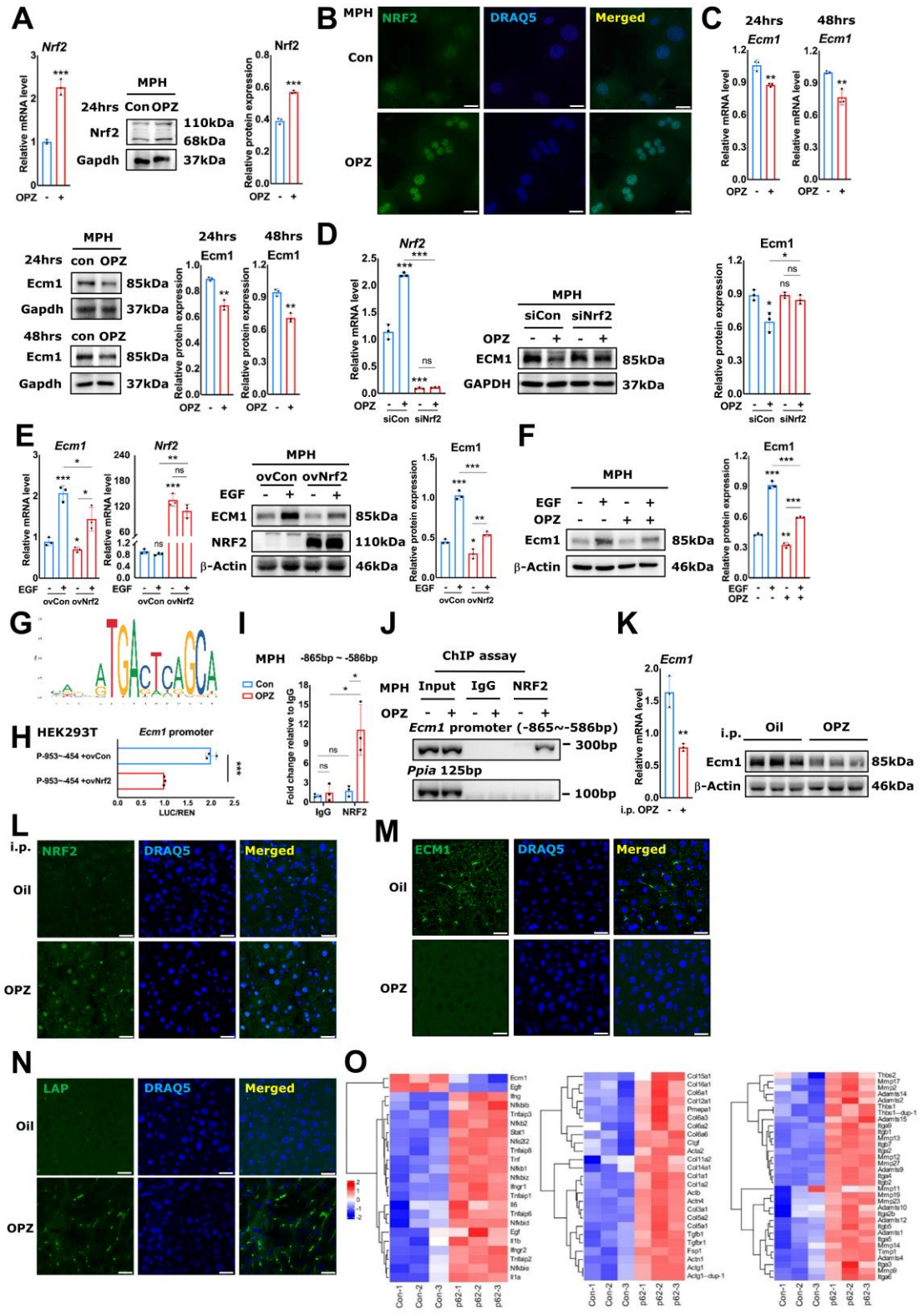
A
Nrf2
Relative mRNA level
OPZ - +
MPH
24hrs Con OPZ
Nrf2 110kDa
68kDa
Gapdh 37kDa
Relative protein expression
B
MPH
NRF2
DRAQ5
Merged
Con
OPZ
C
24hrs
48hrs
Ecm1
Relative mRNA level
D
siCon siNrf2
ECM1 85kDa
GAPDH 37kDa
Relative protein expression
E
ovCon ovNrf2
EGF
ECM1 85kDa
NRF2 110kDa
β-Actin 46kDa
F
G
H
HEK293T
Ecm1 promoter
P-953~-454 +ovCon
P-953~-454 +ovNrf2
LUC/REN
I
MPH -865bp ~ -586bp
Con
OPZ
Fold change relative to IgG
IgG NRF2
J
ChIP assay
MPH Input IgG NRF2
Ecm1 promoter (-865~-586bp)
300bp
Ppia 125bp
100bp
K
i.p. OPZ
i.p. Oil OPZ
L
i.p.
Oil
OPZ
M
ECM1
N
LAP
O
Con-1 Con-2 Con-3 p62-1 p62-2 p62-3

789 **Figure 5. Nrf2 inhibits Ecm1 expression through negative regulatory binding to**
790 **its promoter**
791 **(A)** qRT-PCR and immunoblotting showing the effect of OPZ treatment on Nrf2
792 expression in MPHs. **(B)** Representative immunofluorescence staining for Nrf2
793 expression in OPZ-treated MPHs. Scale bar, 25μm. **(C)** qRT-PCR and immunoblotting
794 displaying the effect of OPZ treatment on Ecm1 expression in MPHs at different time
795 points. **(D)** qRT-PCR and immunoblotting showing the effect of Nrf2 knockdown on
796 Ecm1 expression in OPZ-treated MPHs. **(E)** qRT-PCR and immunoblotting showing
797 the effect of Nrf2 overexpression on Ecm1 and Nrf2 expression in EGF-treated MPHs.
798 **(F)** Immunoblotting displaying the effect of OPZ treatment on Ecm1 expression in
799 EGF-treated MPHs. **(G)** Predicted binding motif of Nrf2 to the *Ecm1* promoter by
800 Jaspar. **(H)** Luciferase reporter assay analyzing the activity of *Ecm1* promoter (-953 ~
801 -454bp) in HEK293T cells transfected with or without Nrf2 plasmid. **(I)** ChIP qRT-PCR
802 showing the effect of OPZ treatment on binding of Nrf2 to the *Ecm1* gene promoter in
803 MPHs. The fragment positions "-865bp ~ -586bp" were calculated relative to the *Ecm1*
804 gene TSS. Rabbit IgG-bound chromatin served as negative control. **(J)** The amplified
805 products of ChIP PCR were separated on 2% agarose gel. *Ppia* represents non-specific
806 binding. **(K)** qRT-PCR and immunoblotting showing the expression of Ecm1 in OPZ-
807 treated mice. Olive oil was administered as placebo. **(L-N)** Representative IF staining
808 showing Nrf2, ECM1 and LAP-D R58 expression in liver tissues from OPZ-treated
809 mice. **(O)** mRNA expression of target genes in liver tissue from p62-KO mice injected
810 with/without adenovirus p62, extracted from the GEO Dataset GSE134188. The results
811 of qRT-PCR are normalized to *Ppia*. Gapdh and β-Actin are loading controls. DRAQ5
812 fluorescent probe stains DNA. Scale bar, 25μm. Quantification of protein expression
813 was done by ImageJ (National Institutes of Health, Bethesda, Maryland, USA). *P*-
814 values were calculated by unpaired Student's t test. Bars represent the mean ± SD. *,
815 $P<0.05$; **, $P<0.01$; ***, $P<0.001$.

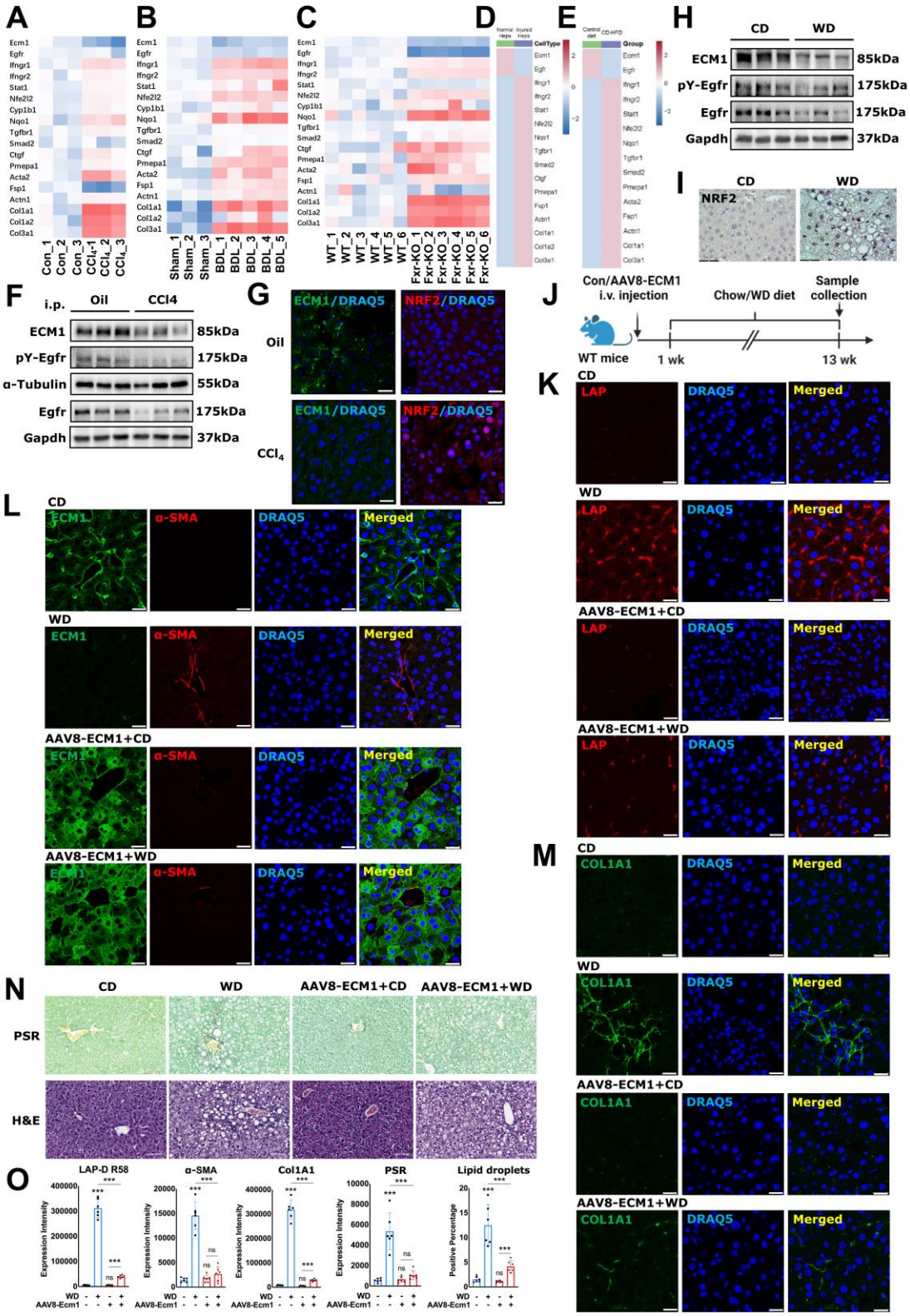
A
B
C
D
E
H
CD
WD
ECM1
pY-Egfr
Egfr
Gapdh
85kDa
175kDa
175kDa
37kDa
I
NRF2
F
i.p.
Oil
CCl4
ECM1
pY-Egfr
α-Tubulin
Egfr
Gapdh
85kDa
175kDa
55kDa
175kDa
37kDa
G
ECM1/DRAQ5
NRF2/DRAQ5
Oil
CCl4
J
Con/AAV8-ECM1
i.v. injection
Chow/WD diet
Sample
collection
WT mice
1 wk
13 wk
K
CD
WD
AAV8-ECM1+CD
AAV8-ECM1+WD
LAP
DRAQ5
Merged
L
CD
WD
AAV8-ECM1+CD
AAV8-ECM1+WD
ECM1
α-SMA
DRAQ5
Merged
M
CD
WD
AAV8-ECM1+CD
AAV8-ECM1+WD
COL1A1
DRAQ5
Merged
N
CD
WD
AAV8-ECM1+CD
AAV8-ECM1+WD
PSR
H&E
O
LAP-D R58
α-SMA
Col1A1
PSR
Lipid droplets
Expression Intensity
Positive Percentage
WD
AAV8-Ecm1

816 **Figure 6. Activation of IFNγ/NRF2 signaling and downregulation of EGFR/ECM1**
817 **in various mouse models of hepatic injury**

818 **(A-E)** Heatmaps of relative mRNA expression for target genes in CCl_4-injured (twice
819 per week for 6 weeks), BDL surgical (7 days after ligation), *Fxr*-KO, DDC diet (for 1
820 week) and CD-HFD fed (for 3 months) mouse models, extracted from the GEO Dataset
821 GSE222576, GSE166867, GSE76163, GSE193850 and GSE232182, respectively. **(F)**
822 Immunoblotting for Ecm1, pY-Egfr and Egfr in liver tissues from oil or CCl_4-treated
823 mice. **(G)** Representative IF staining for Ecm1 and Nrf2 in liver tissues from oil or
824 CCl_4-treated mice. **(H)** Immunoblotting for Ecm1, pY-Egfr and Egfr in liver tissues
825 from CD or WD-fed mice. **(I)** Representative IHC staining for Nrf2 in liver tissues from
826 CD or WD-fed mice. **(J)** Schematic illustration of *in vivo* experiment with AAV8-
827 ECM1 (i.v.) and WD-fed WT mice. **(K-M)** Representative IF staining for LAP-D R58,
828 Ecm1, a-SMA and Col1A1 in liver tissues from CD or WD-fed mice treated with
829 control or AAV8-ECM1. DRAQ5 fluorescent probe stains DNA. Scale bar, 25μm. **(N)**
830 Representative H&E and PSR staining for liver tissues from CD or WD-fed mice
831 treated with control or AAV8-ECM1. Scale bar, 70μm. **(O)** Quantification of staining
832 for LAP-D R58, a-SMA, Col1A1 and PSR, and for lipid droplets according to the white
833 bubbles in the H&E staining. Gapdh, α-Tubulin are loading controls. *P*-values were
834 calculated by unpaired Student's t test. Bars represent the mean ± SD. *, $P<0.05$; **,
835 $P<0.01$; ***, $P<0.001$.

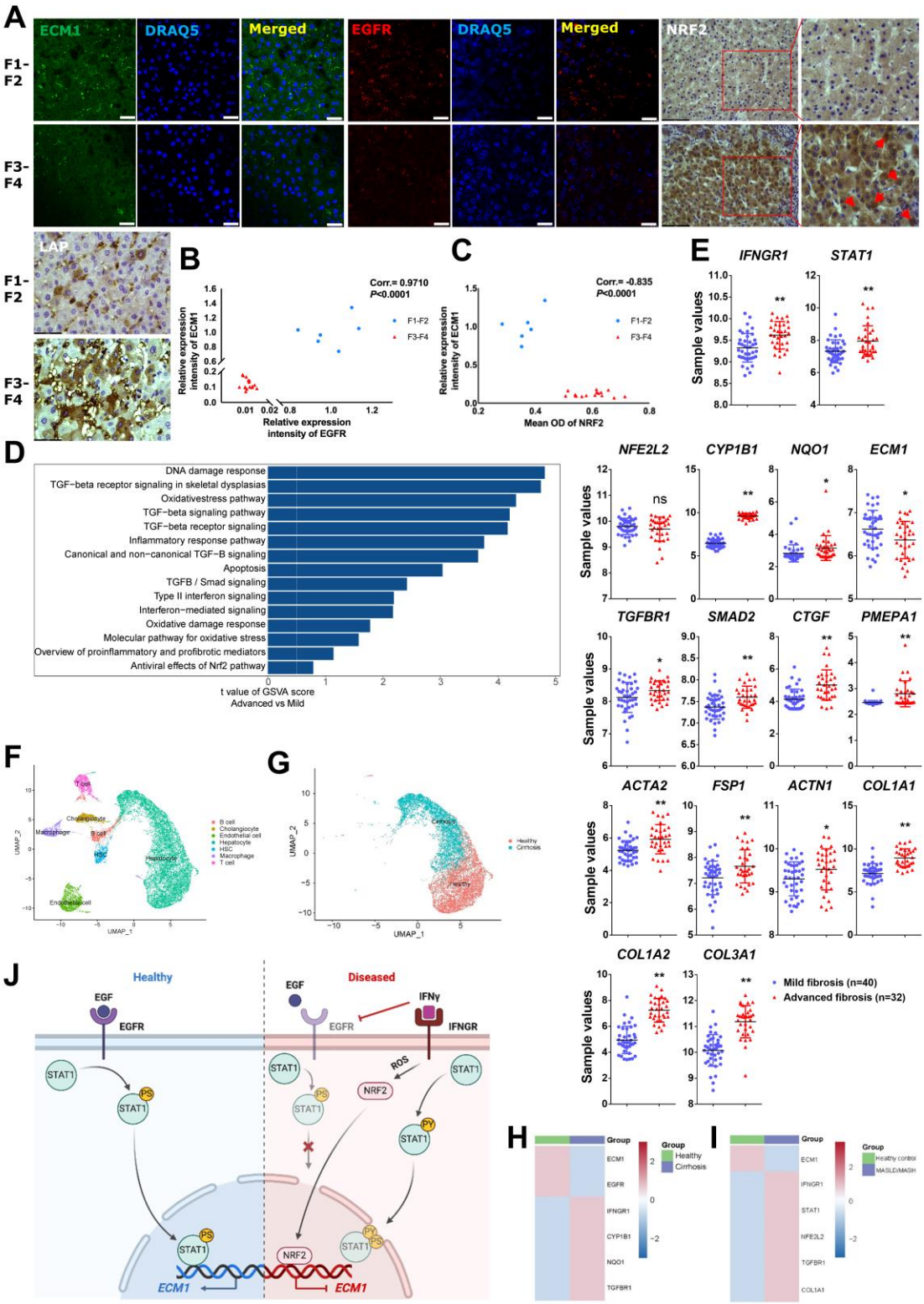
A
ECM1
DRAQ5
Merged
EGFR
DRAQ5
Merged
NRF2
F1-F2
F3-F4
LAP
B
Corr.= 0.9710
P<0.0001
F1-F2
F3-F4
Relative expression intensity of ECM1
Relative expression intensity of EGFR
C
Corr.= -0.835
P<0.0001
Relative expression intensity of ECM1
Mean OD of NRF2
E
IFNGR1
STAT1
Sample values
D
DNA damage response
TGF−beta receptor signaling in skeletal dysplasias
Oxidativestress pathway
TGF−beta signaling pathway
TGF−beta receptor signaling
Inflammatory response pathway
Canonical and non−canonical TGF−B signaling
Apoptosis
TGFB / Smad signaling
Type II interferon signaling
Interferon−mediated signaling
Oxidative damage response
Molecular pathway for oxidative stress
Overview of proinflammatory and profibrotic mediators
Antiviral effects of Nrf2 pathway
t value of GSVA score
Advanced vs Mild
NFE2L2
CYP1B1
NQO1
ECM1
TGFBR1
SMAD2
CTGF
PMEPA1
ACTA2
FSP1
ACTN1
COL1A1
COL1A2
COL3A1
ns
Mild fibrosis (n=40)
Advanced fibrosis (n=32)
F
B cell
Cholangiocyte
Endothelial cell
Hepatocyte
HSC
Macrophage
T cell
UMAP_1
UMAP_2
G
Cirrhosis
Healthy
J
Healthy
Diseased
EGF
EGFR
IFNγ
IFNGR
STAT1
PS
PY
NRF2
ROS
ECM1
H
Group
Healthy
Cirrhosis
ECM1
EGFR
IFNGR1
CYP1B1
NQO1
TGFBR1
I
Healthy control
MASLD/MASH
ECM1
IFNGR1
STAT1
NFE2L2
TGFBR1
COL1A1

836 **Figure 7. Activated IFNγ/NRF2 and decreased ECM1 expression aggravate the**
837 **progression of fibrotic liver diseases**
838 **(A)** Representative IF or IHC staining for ECM1, EGFR, NRF2, and TGF-β1 LAP-D
839 R58 in F1-F2 fibrosis and F3-F4 fibrosis patients. DRAQ5 fluorescent probe stains
840 DNA. Scale bar, IF 25μm, IHC 87μm. **(B-C)** Correlation analysis of EGFR/NRF2 and
841 ECM1 expression levels in the liver tissue of patients with F1-F2 or F3-F4 fibrosis. **(D)**
842 Differences in pathway activity were evaluated using GSVA scores for each patient with
843 advanced (n = 32) and mild liver fibrosis (n = 40). The analysis reports t-values derived
844 from linear models. **(E)** mRNA expression of target genes in liver tissue from patients
845 with F0-F1 or F3-F4 fibrosis, extracted from GEO Dataset GSE49541. **(F, G)** UMAP
846 visualization of cell clusters. **(H)** Analysis of target genes in the hepatocytes from
847 human normal liver (n=2) and MASLD cirrhotic liver (n=2), extracted from scRNA-
848 seq dataset GSE174748. **(I)** Heatmap of target genes expression in MASLD/MASH
849 patients (GSE202379). **(J)** Scheme depicting the regulation of ECM1 expression in
850 hepatocytes in healthy and diseased liver (Figure created with BioRender.com). *P*-
851 values were calculated by unpaired Student's t test. Bars represent the mean ± SD. *,
852 $P<0.05$; **, $P<0.01$; ***, $P<0.001$.